AD-A149 334 A STUDY OF THE K-EDGE ABSORPTION SPECTRA OF SELECTED VANADIUM COMPOUNDS(U) GENERAL ELECTRIC CO SCHENECTADY N Y J WONG ET AL. 15 NOV 84 TR-1 N00014-83-C-0620 1/1

UNCLASSIFIED F/G 7/4 NL

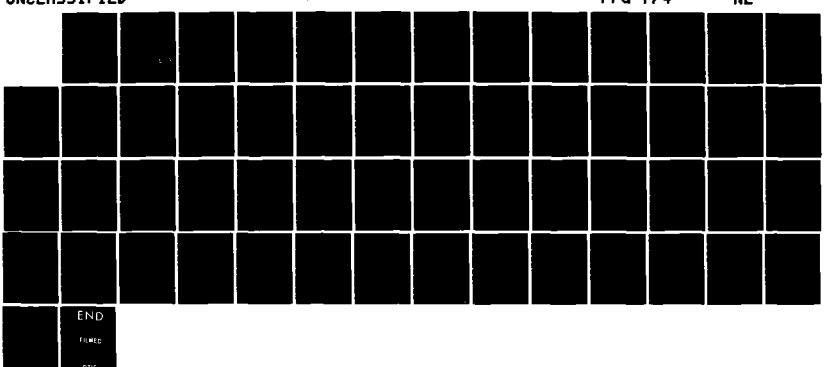

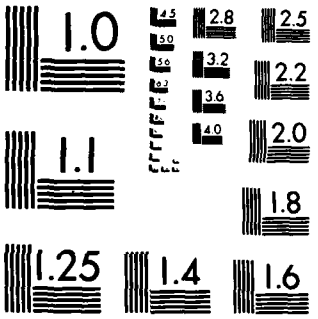

Office of Naval Research

Contract N 00014-83-C-0620

Technical Report No. 1

A Study of the K-edge Absorption Spectra of Selected Vanadium Compounds

by

J. Wong*, F. W. Lytle**, R. P. Messmer* and D. H. Maylotte*

Submitted to Physical Review B

*General Electric Corporate Research & Development
P. O. Box 8, Schenectady, NY 12301

**The Boeing Company, Seattle, WA 98124

15 November 1984

SECURITY CLASSIFICATION OF THIS PAGE (When Data Entered)

REPORT DOCUMENTATION PAGE		READ INSTRUCTIONS BEFORE COMPLETING FORM
1. REPORT NUMBER 1	2. GOVT ACCESSION NO. AH49334	3. RECIPIENT'S CATALOG NUMBER
4. TITLE (and Subtitle) A Study of the K-edge Absorption Spectra of Selected Vanadium Compounds		5. TYPE OF REPORT & PERIOD COVERED Technical Report 6. PERFORMING ORG. REPORT NUMBER
7. AUTHOR(s) J. Wong, F. W. Lytle*, R. P. Messmer and D. H. Maylotte		8. CONTRACT OR GRANT NUMBER(s) N 00014-83-C-0620
9. PERFORMING ORGANIZATION NAME AND ADDRESS *The Boeing Co., Seattle, WA 98124		10. PROGRAM ELEMENT, PROJECT, TASK AREA & WORK UNIT NUMBERS
11. CONTROLLING OFFICE NAME AND ADDRESS Office of Naval Research 800 N. Quincy Street Arlington, VA 22217		12. REPORT DATE November 1984 13. NUMBER OF PAGES Unclassified
14. MONITORING AGENCY NAME & ADDRESS(if different from Controlling Office)		15. SECURITY CLASS. (of this report) 15a. DECLASSIFICATION/DOWNGRADING SCHEDULE

16. DISTRIBUTION STATEMENT (of this Report)

Approved for public release; distribution unlimited

17. DISTRIBUTION STATEMENT (of the abstract entered in Block 20, if different from Report)

18. SUPPLEMENTARY NOTES

19. KEY WORDS (Continue on reverse side if necessary and identify by block number)

Vanadium, X-ray Absorption Spectra,
X-ray Absorption Near Edge Structure (XANES)

20. ABSTRACT (Continue on reverse side if necessary and identify by block number)

High resolution vanadium K-edge absorption spectra have been recorded for a number of selected vanadium compounds of known chemical structure using synchrotron radiation available at the Stanford Synchrotron Radiation Laboratory (SSRL). The compounds studied include oxides: VO, V_2O_3, V_2O_7, V_2O_4, and V_2O_5; vanadates: NH_4VO_3, $CrVO_4$, and $Pb_5(VO_4)_3Cl$; vanadyl compounds:

DD FORM 1 JAN 73 1473 EDITION OF 1 NOV 65 IS OBSOLETE
S/N 0102-LF-014-6601

Unclassified
SECURITY CLASSIFICATION OF THIS PAGE (When Data Entered)

$VOSO_4 \cdot 3H_2O$, vanadyl bis 1-phenyl 1,3-butane dionate, vanadyl phthalocyanine and vanadyl tetraphenylporphyrin; intermetallics: VH, VB_2, VC, VN, VP, and VSi_2; V_2S_3 and a vanadium-bearing mineral, roscoelite. Vanadium in these compounds exhibits a wide range of formal oxidation states (0 to +5) and coordination geometries (octahedral, tetrahedral, square pyramid, etc.) with various ligands. The object of this systematic investigation is to gain further understanding of the details of various absorption features in the vicinity of the K absorption edge of a constituent element in terms of its valence, site symmetry, coordination geometry, ligand type, and bond distances. In particular the intensity and position of a well-defined pre-edge absorption in some of these compounds have been analyzed semi-quantitatively within a molecular orbital framework and a simple coordination charge concept.

A STUDY OF THE K-EDGE ABSORPTION SPECTRA OF SELECTED VANADIUM COMPOUNDS

J. Wong, F. W. Lytle*, R. P. Messmer, and D. H. Maylotte

General Electric Corporate Research and Development
P.O. Box 8, Schenectady, NY 12301

*The Boeing Company, P.O. Box 3999, 2T-05 Seattle, WA 98124

Abstract

High resolution vanadium K-edge absorption spectra have been recorded for a number of selected vanadium compounds of known chemical structure using synchrotron radiation available at the Stanford Synchrotron Radiation Laboratory (SSRL). The compounds studied include oxides: VO, V_2O_3, V_4O_7, V_2O_4, and V_2O_5; vanadates: NH_4VO_3, $CrVO_4$, and $Pb_5(VO_4)_3Cl$; vanadyl compounds: $VOSO_4 \cdot 3H_2O$, vanadyl bis 1-phenyl 1,3-butane dionate, vanadyl phthalocyanine and vanadyl tetraphenylporphyrin; intermetallics: VH, VB_2, VC, VN, VP, and VSi_2; V_2S_3 and a vanadium-bearing mineral, roscoelite. Vanadium in these compounds exhibits a wide range of formal oxidation states (0 to +5) and coordination geometries (octahedral, tetrahedral, square pyramid, etc.) with various ligands. The object of this systematic investigation is to gain further understanding of the details of various absorption features in the vicinity of the K absorption edge of a constituent element in terms of its valence, site symmetry, coordination geometry, ligand type, and bond distances. In particular the intensity and position of a well-defined pre-edge absorption in some of these compounds have been analyzed semi-quantitatively within a molecular orbital framework and a simple coordination charge concept.

A STUDY OF THE K-EDGE ABSORPTION SPECTRA OF SELECTED VANADIUM COMPOUNDS

J. Wong, F.W. Lytle*, R.P. Messmer, and D.H. Maylotte

General Electric Corporate Research and Development

P.O. Box 8, Schenectady, NY 12301

*The Boeing Company, P.O. Box 3999 2T-05, Seattle, WA 98124

I. Introduction

As the region near an x-ray absorption edge is scanned in energy, the ejected photoelectron sequentially probes the empty electronic levels of the material. The resulting x-ray absorption near-edge structure (XANES) within 30 eV of threshold have long been known to be rich in chemical and structural information.[1,2] An attempt to correlate a large number of XANES spectra for transition metal and post-transition metal oxides, including those of vanadium, was made by White and McKinstry.[3] Reconciliations of molecular orbital theory with XANES spectra were made by Best[4] for tetrahedrally coordinated oxy-complexes of transition metals, by Seka and Hanson[5] for octahedral complexes, and by Fischer[6] and Tsutsumi et al.[7] for Ti and V compounds. Also, Fischer and Baun[8] have taken an alternate approach using calculated band structures[9,10] for Ti, its oxides, nitride, carbide, and boride to correlate the Ti $L_{3,2}$ spectra from these materials.

All of the earlier efforts suffered from the (varying) poor resolution of their experiments. With the availability of intense and well collimated synchrotron x-radiation sources, these spectra can now be measured more quickly,

simply and with greater resolution than ever before. A number of interesting papers have recently been published on K-edge[11-19] and L-edge[20-22] spectra measured with synchrotron sources. For K-edge spectra of transition metal compounds there are generally weak but distinct absorption features just before the onset of the main absorption edge. These features have been attributed by Shulman et al.[11] to electronic transitions from 1s to nd, ns (non-dipole) and to np (dipole-allowed) empty states. For L-edge absorption, the transitions are from 2s and 2p to some higher empty p and s or d states respectively.[23] Recently, the linearly polarized characteristic of synchrotron radiation has been used to determine the orientation dependence of the K-edge spectra in single crystals[24,25] and enabled certain types of geometric information about the x-ray absorbing species to be deduced.

Vanadium exhibits a wide range of oxidation states (-1,0,...+5) and coordination geometries (octahedral, tetrahedral, square pyramid, trigonal bipyramidal as well as dodecahedral) with various ligands in its compounds.[26] This richness in chemical structures gives rise to a number of outstanding absorption features in the vicinity of the V K-edge[3,27,28] and L-edge[29] that are useful in systematic study and understanding of the effect of bonding and coordination symmetry on the observed XANES[30] spectra. In this study we utilize synchrotron radiation from the Stanford Positron Electron Accelerator Ring (SPEAR) available at SSRL to obtain high resolution K-edge XANES spectra of vanadium in a series of selected compounds of well-defined coordination geometry and known bond distances. The intensity and position of the near-edge spectral features are analyzed within a quantum molecular orbital framework and a simple coordination charge concept. The XANES spectra of these compounds have also been used to model and elucidate the V sites in tunicate

blood cells,[31] in coal,[32] and in crude oil.[33]

II. Experimental

The compounds studied in the present investigation include the vanadium oxides: VO, V_2O_3, V_4O_7, V_2O_4, and V_2O_5; vanadates: NH_4VO_3, $CrVO_4$, and $Pb_5(VO_4)_3Cl$ (the mineral vanadinite); vanadyl compounds: $VOSO_4 \cdot 3H_2O$, vanadyl bis 1-phenyl 1,3-butane dionate (VOPBD), vanadyl phthalocyanine (VPc) and vanadyl tetraphenylporphyrin (VTPP); intermetallics: VB, VB_2, VC, VN, VP, and VSi_2; V_2S_3 and another vanadium-containing mineral: roscoelite $KAlV_2Si_3O_{10}(OH)_2$. The compounds VO, VB_2, and V_2S_3 were purchased from Cerac Inc., the vanadyl compounds from Eastman Kodak, NH_4VO_3 from Fischer Scientific, the two minerals from Ward's Natural Science Establishment, Rochester, NY, and the remaining materials from Alfa Inorganic Chemicals. Phase purity of all the inorganic compounds and the two minerals was checked by in-house powder diffraction to be better than 98%. The organic vanadyl compounds were Kodak certified.

Spectral samples for transmission study were prepared by mulling -400 mesh powders of vanadium compounds with Duco cement,[34] squeezing the mull between two 2" X 3" microscope slides to obtain a uniform thickness and subsequent gliding the slides apart to allow the films to cure in air. Details of the casting procedure will be described elsewhere.[35] The cast films were allowed to cure for about 30 minutes and then removed from the microscope slides with a sharp razor blade. The concentration of the powder in the mull and thickness of the film were manipulated so as to provide 1 to 2 absorption lengths of the material at an energy just above the vanadium K-edge with the

use of a single or a duplex film.

Room temperature vanadium K-edge absorption spectra were measured with the EXAFS I-S spectrometer at SSRL during a dedicated run of SPEAR at an electron energy of 3 GeV and storage ring current of ~ 100 mA. The synchrotron x-ray beam from SPEAR was monochromatized with a channel-cut Si(220) crystal and a 1-mm entrance slit, which yielded a resolution of approximately 0.3 eV at 5 KeV. Spectra were recorded in four energy regions about the V K-edge at ~ 5465.0 eV: -100 eV to -50 eV in 10 eV steps; -50 eV to +50 in 0.5 eV steps; 50 eV to 500 eV in 3 eV steps and 500 eV to 1000 eV in 7 eV steps. This scanning procedure yielded quality data of both pre-edge and post-edge (EXAFS) backgrounds for subsequent normalization of the XANES spectra. Calibrations of the spectrometer were made before, between and after scanning various vanadium compounds using a 5 μm thick (2.5 absorption lengths) vanadium metal foil.[36] The concentration of vanadium in VPc, VTPP and roscoelite was only a few percent by weight. Spectral specimens of these materials were made by simply packing the powder in 6 μm polypropylene bags and their spectra were taken with a fluorescence technique[37] using a Ti-filter ion-chamber assembly described elsewhere.[32,38]

III. Results and Discussion

III.A Normalized XANES and Derivative Spectrum

In order to compare quantitatively the intensity of absorption features in various vanadium compounds the experimental K-edge spectra were normalized. The procedure is illustrated graphically in Fig. 1 for the case of vanadium metal. The solid curve is the raw experimental data plotted as $A = \ln(\frac{I_o}{I})$

versus energy. The pre-edge region AB (-100 eV to -10 eV) is linearly fitted and extrapolated above the edge energy to C. The post-edge (EXAFS) background XY from 50-100 eV was determined by using a cubic spline fit procedure with three equal segments and extrapolating below the edge energy to Z. The absorption jump is given by PQ at E=0. The zero of energy is taken with respect to the first inflection point of the vanadium metal in the derivative spectrum at 5465.0 eV, which marks the threshold or onset of photo-ejection of the 1s electron in vanadium metal.[36] The derivative spectrum within ±70 eV of the K-absorption edge is shown in Fig. 2(a) and was obtained by drawing through points given by:

$$\frac{dA}{dE} = \frac{A(E + \Delta)-A(E)}{\Delta} \qquad (1)$$

with Δ the energy step size of the absorption spectrum. This derivative spectrum and those shown later in Figs. 4, 7, 9, 11, and 13 are characterized by a well-defined and intense peak at the onset of photo-ejection in the region 0-5 eV. This feature is followed by a number of strong and narrow peaks to about 30 eV, defining the XANES region. At higher energies, structures in the derivative spectrum are much broader and lower in intensity, characteristics of the EXAFS oscillations. Thus, the derivative spectrum may be used operationally to separate the XANES and EXAFS regions of the experimental x-ray absorption spectrum.[38a]

The normalized XANES spectrum was obtained by subtracting the smooth pre-edge absorption AB from every point in the experimental spectrum in Fig. (1) in the range ±70 eV and dividing by the step height PQ at E=0. As seen in Fig. 2(b), the normalized K-edge XANES spectrum of bcc vanadium metal is characterized by a sharp absorption peak at 1 eV, a shoulder at 6 eV, followed by a steep-rising edge (the main absorption edge at ~10 eV) that leads to

various well-defined peaks at 19.2 eV, 28.8 eV and others at higher energy in the EXAFS (extended x-ray absorption fine structure) region. The inflection point associated with each of these absorption features shows up more clearly as a peak in the derivative spectrum which facilitates the enumeration as well as location of the absorption features particularly those on the rising edge of the XANES spectrum.

In the following sections, the K-edge XANES spectra of vanadium in the oxides, in octahedral, square pyramidal and tetrahedral coordination will be presented and discussed in some detail. Spectra of some vanadium intermetallic compounds will also be presented and discussed.

III.B Vanadium Oxides

Vanadium forms a series of oxides over a range of formal oxidation state (valence).[39] The crystal structures of VO, V_2O_3, V_4O_7, V_2O_4, and V_2O_5 are known. These oxides provide a useful series of materials for systematic study of the effects of valence and coordination geometry on the XANES spectrum of the central metal atom coordinated by the same ligand. VO has a NaCl structure with regular octahedral VO_6 units.[40] V_2O_3 has a corundum structure in which V^{3+} ions are six-fold coordination by oxygen ions at two distinct distances of 1.96 Å and 2.06 Å.[41] V_4O_7 is a mixed valence oxide consisting of both V^{3+} and V^{4+} ions. The structure consists of a distorted hexagonal close-packed oxygen array with vanadium atoms occupying the octahedral sites (distorted) so as to form rutile blocks which extend indefinitely in the triclinic a-b plane. The rutile blocks are four octahedra thick along the perpendicular to this plane. There are four crystallographic non-equivalent vanadium sites with V-O distances ranging from 1.883 to 2.101 Å.[42] The crystal structure

of V_2O_4 is monoclinic and is a distorted form of rutile.[43] The V atoms are again six-fold coordinated by oxygens, but is much displaced from the center of the octahedron resulting in a short V-O bond of 1.76 Å. In V_2O_5, the V is five-fold coordinated in a distorted tetragonal pyramid of oxygen.[44] The apex oxygen distance is only 1.585 Å whereas the basal V-O distances vary from 1.78 to 2.02 Å. The site symmetry of the V atom decreases from O_h in VO to C_3 in V_2O_3, C_1 in both V_4O_7, and V_2O_4, and C_s in V_2O_5. The relevant structural parameters of these oxides and other compounds studied here are summarized in Table I.

The spectra of Fig. 3 show that the V K-edge XANES in these oxides exhibit a pre-edge absorption feature which grows in intensity in going from V_2O_3 to V_2O_5, followed by a weak shoulder on a rising absorption curve (the absorption edge) which culminates in a strong peak in the vicinity of ~20 eV. This strong peak has been assigned by Shulman et al.[11] and Hu et al.[14] as the allowed transition 1s → 4p, the lower energy shoulder as the forbidden transition 1s → 4s and the pre-edge feature at threshold as the forbidden transition 1s → 3d. At energies equal to and above the 1s → 4p transition absorption features may arise from transition to higher np states, shape resonances[45-47] and/or multiple scattering[48,49]. The latter two effects are much more complicated to analyze.

Since the initial 1s state is a gerade state, the 1s → 3d transition is strictly dipole forbidden as it is in the case with VO which contains regular octahedral VO_6 units having a center of inversion. When the symmetry of the liganda is lowered from O_h, the inversion center is broken as in the case of V_2O_3, V_4O_7, and V_2O_4 with distorted octahedral VO_6 groups; and in V_2O_5 with distorted square pyramidal VO_5 groups. The pre-edge absorption becomes dipole

allowed due to a combination of stronger 3d–4p mixing and overlap of the metal 3d orbitals with the 2p orbitals of the ligand.[11]

The intensity variation of the pre-edge peak across the oxide series is noteworthy. As seen in Fig. 3 the oscillator strength increases with progressive relaxation from perfect octahedral symmetry (as in VO) to distorted octahedral VO_6 groups as in (V_2O_3, V_4O_7, V_2O_4) and to a lower coordination with a short V-O bond (see Table 1) in a square pyramidal symmetry (as in V_2O_5). The "molecular cage" effect on the oscillator strength of this transition to the 3d orbitals in K-edge spectra as noted by Kutzler et al.[50] appears to be operative here. We shall discuss the cage size effect in more detail in Section III.G in conjunction with other vanadium compounds which also exhibit a strong 1s → 3d pre-edge transition.

Closer examination of the spectrum of V_2O_3 shows that there is a multiplet structure in the pre-edge peak region. The multiplet structure which shows splitting of ~1.3 eV and ~2.0 eV can be seen more clearly in the corresponding derivative spectrum in Fig. 4. The splittings in the 1s → 3d transition is caused by crystal field splitting of the ground state,[11] and in the case of V_2O_3 the d levels of V^{3+} ions in C_3 site are split into A + 2E. A similar triplet pre-edge structure is also observed in roscoelite and V_2S_3 as well as in other transition metal compound with similar crystal symmetry such as TiO_2.[18] (See following section). A doublet splitting is also evident in the case of V_2O_5 shown in Fig. 4.

The energy positions of various absorption features are found to be correlated with the oxidation state (formal valency) of V in the oxides. The experimental data are summarized in Table 2. With increase in oxidation

state, (a) the absorption threshold as defined by the position of the first peak in the derivative spectrum, (b) the absorption edge as defined by the second peak in the derivative curve, (c) the energy of the pre-edge peak, and (d) the 1s → 4p transition above the absorption edge all shift to higher energies. The energy shifts, so-called chemical shifts are found to follow Kunzl's law[51,52] and vary linearly with valence of the absorbing vanadium atom as shown in Fig. 5. The positive shift in the threshold energy with valence increase can be understood conceptually to be due to an increase in the attractive potential of the nucleus on the 1s core electron and a reduction in the repulsive core Coulomb interaction with all the other electrons in the compound. The lines in Fig. 5 are least-squares fitted lines with slopes of 1.4, 1.1, 2.5, and 3.2 eV per valence increase for the threshold, pre-edge peak, the absorption edge and the 1s → 4p transition respectively. The increase in slope merely reflects tighter binding of the inner 3d and 4s levels with respect to the outermost 4p levels which are more easily perturbed by valence change.

Finally a comparison with earlier data on these oxides is in order. A number of K-edge absorption studies have been reported using x-ray tube sources.[3,27,28] All of these earlier studies failed to measure many of the narrow spectral features in both the pre-edge and edge regions because of the poor resolution of their experiments. For example the pre-edge peaks for V_4O_7 and V_2O_4 shown in Fig. 3 were not resolved and that for V_2O_5 was severely suppressed in intensity.[3,27,28] Sample over-thickness and phase purity contributed to the sources of differences. The structureless absorption feature above the K-edge in V_2O_5 was attributed to a lack of octahedral symmetry of the V center,[28] which is not so as shown in Fig. 3. This was an artifact

due to sample over-thickness in a transmission experiment. In the same study,[28] a pre-edge peak not expected of V in perfect octahedral symmetry was recorded for VO. The sample in all likelihood was contaminated with V_2O_5.

III.C V in Octahedral Coordination

Roscoelite is a one-layer monoclinic mica in which the Al^{3+} ions in the octahedral AlO_6 sheet are partially substituted (~17%) by V^{3+} ions which occupy distorted octahedral sites.[53] The V K-edge spectrum of roscoelite is shown in Fig. 6 and is qualitatively similar to that in pure V_2O_3. The pre-edge absorption in roscoelite again exhibits a triplet feature but is more intense and much better resolved than that in V_2O_3. The normalized peak intensity of the 1s → 4p transition above the edge at 21.5 eV is also higher (>1.4), indicating a larger emptiness of the final p state in roscolite induced by the smaller and more polarizing next-nearest Al^{3+} neighbor compared with pure V_2O_3.

V_2S_3 is also monoclinic[54,55] but the crystal structure has not been determined. Its V K-edge XANES is also plotted in Fig. 6 and bears general resemblance to those of V_2O_3 and roscoelite, suggesting that V^{3+} are six-fold coordinated by $S^{=}$ in a distorted octahedral environment. The positions of the threshold, pre-edge peak, edge and 1s → 4p transition are quite similar to those of V_2O_3 and roscoelite (see Table 2). The triplet pre-edge feature is better seen in the derivative spectrum shown in Fig. 7. Compared with V_2O_3 and roscoelite the 1s → 4p transition in V_2S_3 is broader and lower in peak intensity. This may be due largely to a ligand (electronegativity) effect to be discussed later in Section III.H.

III.D V in Tetragonal Square Pyramidal Coordination

Five-fold coordination is typical of a number of vanadyl compounds containing a short V-O bond at a distance of ~1.6 Å. Vanadium in these compounds generally is tetravalent, although pentavalent vanadium compounds such as V_2O_5 and the oxyhalides of vanadium (VOX_3, X=F,Cl or Br) are also known to have a short V-O bond.[26] In Fig. 8, the K-edge spectra of a series of vanadyl compounds are shown. The respective formal valence, bond type and nearest neighbor bond distances are given in Table 1. Like V_2O_5, the XANES spectra of these compounds are typified by a strong 1s → 3d pre-edge absorption. The energy position of this pre-edge peak, as well as those of the absorption threshold, absorption edge and the 1s → 4p transition are summarized in Table 2. In VOPBD[56] vanadium is tetravalent and is coordinated by oxygens at distances of 1.61 Å, 1.95 Å, and 1.98 Å. In VTPP[57,58] and VPc[59] vanadium is also tetravalent. The basal plane of the square pyramids is now replaced by nitrogen ligands. As seen from the bond distances given in Table 1, the tetragonal pyramid unit in both the porphyrin and phthalocyanine compounds is more regular than that in VOPBD, and consists primarily of a single distance to the basal ligands. However, there is a discernible difference between these two compounds: both the V-O and V-N distances in the phthalocyanine are shorter than those in the porphyrin compound. This difference in bond distance appears to correlate with the intensity of the pre-edge 1s → 3d absorption, again indicative of a "molecular cage size" effect. The smaller the cage, the higher the intensity of this transition as in the case of VPc.

In $VOSO_4 \cdot 3H_2O$ the tetravalent vanadium center is essentially five-fold coordinated by a short vanadyl oxygen at 1.56 Å, two oxygens from 2 $SO_4^=$ groups at 2.02 Å and 2 more oxygens from 2 water molecules of hydration at 2.06 Å.

However, there is a sixth oxygen from a third water molecule at a further distance of 2.28 Å.[60] This situation is similar to V_2O_5, in which case the sixth oxygen is yet at a further distance of 2.78 Å from a VO_5 unit below, and is too far to be considered in the primary coordination sphere.[44] It is interesting to note that, like V_2O_5, $VOSO_4 \cdot 3H_2O$ also exhibits a weak shoulder on the low energy side of the pre-edge peak. The shoulder feature is easily discernible in the derivative spectra of $VOSO_4 \cdot 3H_2O$ shown in Fig. 9 and Fig. 4 for V_2O_5.

III.E V in Tetrahedral Coordination

The intense dipole-allowed absorption occurring in the pre-edge region of K-edge spectra of transition metals in $CrO_4^{=}$[4], MnO_4^{-}[17], $MoO_4^{=}$[52], $MoS_4^{=}$[52], and more recently TiO_4 units[18] is well known. The presence of this absorption is diagnostic of a tetrahedral environment of the x-ray absorbing transition metal. This characteristic pre-edge absorption is also found in K-edge spectra of vanadium in four-fold coordination. In Fig. 10 a series of V K-edge XANES spectra are shown for the cases of NH_4VO_3, $CrVO_4$, and $Pb_5(VO_4)_3Cl$ vanadinite mineral. Vanadium is pentavalent in these compounds. The energy positions associated with various absorption features in the XANES are similar to those of V_2O_5 (see Table 2).

NH_4VO_3 is a metavanadate isostructural with KVO_3, space group Pmab with Z=4 per unit cell.[61] The structure consists of tetrahedral VO_4 chains similar to those in diopside $CaMg(SiO_3)_2$. However, there are two types of V-O bonds in the tetrahedral chain. Within the VO_4 tetrahedron two bonds are formed with oxygen atoms which link the tetrahedra together and have a V-O distance of 1.81 Å. The other two bonds are formed with terminal (unlinked)

oxygens in the mirror plane and have a shorter V-O distance of 1.66 Å. Asymmetry of the vanadium tetrahedron has been ascribed to the tendency of V to form multiple bonds with oxygens.[61]

$CrVO_4$ is also orthorhombic, space group Cmcm with Z=4 per unit cell.[62,63] Since V and Cr have very similar atomic scattering factors, x-ray diffraction measurements have not been able to locate correctly the V and Cr atoms in the structure. By using the characteristic pre-edge absorption, Lytle[64] showed that the Cr K-edge in $CrVO_4$ did not exhibit a pre-edge line whereas the V edge did, and concluded that V is in the four-fold coordinated C_{2v} sites and Cr in the six-fold coordinated C_{2h} sites of the structure. Like NH_4VO_3, there exists two V-O distances in $CrVO_4$ at 1.72 Å and 1.80 Å, the difference of which is smaller than that in NH_4VO_3.

Vanadinite $Pb_5(VO_4)_3Cl$ is a mineral isostructural with fluorapatite.[65] In this compound the pentavalent V center is four-fold coordinated with oxygens and takes the place of phosphorus in the apatite structure. No crystal structure determination has been made of this mineral. The V-O bond distance was estimated to be ~1.75 Å.[66] The width of the pre-edge peak is narrowest for the mineral, being 2.2 eV compared with 3.0 eV and 3.5 eV for $CrVO_4$ and NH_4VO_3 respectively. The width may be correlated with the spread of V-O distances in the various VO_4 tetrahedra: 0.15 Å in NH_4VO_3 and 0.08 Å in $CrVO_4$. Extrapolating, it is likely that the V-O bond distance in $Pb(VO_4)_3Cl$ is single-valued. The sharpness of the pre-edge peak is also reflected in the derivative spectra shown in Fig. 11. In fact, the weak shoulder on the low energy side of the pre-edge absorption for NH_4VO_3 is clearly brought out in Fig. 11.

III.F V Intermetallic Compounds

Vanadium forms alloys and intermetallic compounds with a large number of elements.[67] We have measured several intermetallic compounds of V with the light elements: VH, VB_2, VC, VN, VP, and VSi_2. The normalized XANES spectra are shown in Fig. 12 and the corresponding derivative curves are shown in Fig. 13.

VH has a body-center tetragonal structure,[68] but details of the atomic arrangement within the unit cell have not been determined. The V K-edge spectrum of this hydride is rather structureless consisting essentially of an absorption edge. Weak absorptions on the rising part of the edge are discernible only in the derivative spectrum.

VB_2 belongs to the space group D^1_{6h} with Z=1 per unit cell.[69] The V and B atoms occupy D_{6h} and D_{3h} sites, and lie in alternate planar layers in the the hexagonal structure. Each V has 6 equidistant closest metal neighbors in its plane, and 12 equidistant B neighbors, 6 in the layer above and 6 in the layer below the metal atom. The existence of a center of inversion symmetry precludes a 1s $\rightarrow$ 3d type transition in the pre-edge region.

VC[70] and VN[71] have the same NaCl structure as VO. The near-edge spectrum of the latter has been plotted in Fig. 3. VP has a NiAs structure with V atoms in D_{3d} sites.[72] The spectra of the intermetallics VC, VN, and VP exhibit a pre-edge absorption, and in the case of VC, a pre-edge peak at 5.4 eV is well resolved. Since there exists a center of inversion in both O_h and D_{3d} symmetries, the 1s $\rightarrow$ 3d transition is dipole forbidden and is only quadrupole allowed (but with low intensity). The experimental intensities of the pre-edge absorption in both VN and VC are quite high when compared with

those of V_2O_3, V_2S_3 and roscoelite, which are shown in Fig. 6. Also, it is noted that the intensity of the pre-edge peak increases in going through the series VO, VP, VN, and VC and may be correlated with the character of the unoccupied states above the Fermi level which become less metal-like and more ligand-like.[73].

VSi_2 belongs to space group D_6^5 with Z=3 per unit cell.[74] V atoms are situated in C_2 sites in the structure. In the region of 5-25 eV the V K-edge spectrum exhibits a multitude of unresolved absorptions, which can be enumerated more easily in the corresponding derivative spectrum of Fig. 13.

The energy positions of the absorption threshold, the edge and 1s $\rightarrow$ 4p transition for these intermetallic compounds are given in Table 2. In general these energies are lower than those of the oxides and other compounds discussed in the preceeding sections. The XANES spectra of these intermetallics vary from being rather featureless such as that of VH to being rather complex such as that of VSi_2.

III.G Intensity of the Pre-Edge Absorption

As seen in the preceding sections, the pre-edge absorption is an outstanding feature in the K-edge XANES spectra of vanadium in a number of the compounds selected for this study. Empirically the strength of this pre-edge transition is found to be dependent on the size of the "molecular cage" defined by the nearest-neighbor ligands coordinating to the x-ray absorbing vanadium center. This correlation is illustrated in a series of plots of the observed intensity versus a cage size parameter. In Fig. 14, the intensity was obtained as the product of the normalized peak height and width at half height, $\nu_{1/2}$. The cage size parameter was defined as an average bond distance,

$\overline{R} = 1/n \sum_{i}^{n} R_i$ where n = number of nearest-neighbor bonds given in Table 1. In Fig. 14, for each geometry type it is clear that the smaller the "molecular cage", the higher the intensity of the pre-edge absorption. This has been noted qualitatively in the preceeding sections. Here an attempt is made to obtain theoretical foundation, within a quantum mechanical framework, for this intensity variation with cage size. Ideally, the theoretical explanation should be independent of cage geometry and therefore be more general than the correlation empirically given in Fig. 14.

For K-edge XANES, the pre-edge absorption is due to a transition from an initial 1s state, ϕ_{1s}, of the central x-ray absorbing vanadium atom to some final molecular orbital state, ϕ_f, of the vanadium-ligand cluster. ϕ_f may be given as a linear combination of the appropriate atomic orbitals ϕ_i's which include the 2p orbitals of the oxygen and/or nitrogen ligands:

$$\phi_f = \sum c_i \phi_i \tag{2}$$

In the dipole approximation, the matrix element associated with the transition is

$$\langle \phi_f | M | \phi_{1s} \rangle = \sum c_i \langle \phi_i | M | \phi_{1s} \rangle \tag{3}$$

where M is the dipole operator. The intensity, I, is proportional to the square of the matrix element,

$$I \propto \left| \sum c_i \langle \phi_f | M | \phi_{1s} \rangle \right|^2 \tag{4}$$

Using the Slater-type orbitals (STO) expression derived by Wahl, Cade, and Roothaan[75] for the one-electron two center molecular integrals, Equation (4) may be approximated by

$$I \propto \left| \sum c_i R_i^2 \exp(-\zeta_i R_i) \right|^2 \tag{5}$$

where c_i are the LCAO coefficients such that $\sum c_i^2 = 1$, R_i is the bond distance of the i^{th} ligand in Bohr units and ζ_i are the atomic orbital exponents. A large value of ζ_i implies a fast decay of the orbital away from the nucleus, i.e. a localized orbital.

Rewriting Equation (5) using a two-term expression on the right-hand side which includes only the short vanadyl bond, R_1, and the average, R_2, of the remaining longer vanadium-ligand distance for the vanadium compounds studied here, we obtain

$$I \alpha \left[c_1(\gamma R_1)^2 \exp(-\zeta \gamma R_1) + c_2(\gamma R_2)^2 \exp(-\zeta \gamma R_2)\right]^2 \qquad (6)$$

where $\gamma = 1.89$ Bohr units/Å and R_1 and R_2 are now in Å. Equation (6) is designed to evaluate the effect of the short V-O bond on the observed pre-edge intensity. A plot of ln I versus ln $\left[c_1(\gamma R_1)^2 \exp(-\zeta \gamma R_1) + c_2(\gamma R_1)^2 \exp(-\zeta \gamma R_2)\right]$ should yield a theoretical slope of 2 for a proper choice of c_1, c_2, and ζ.

A series of systematic iterations was undertaken to calculate the slope of ln I versus ln [RHS of Equation (6)] using the observed pre-edge intensity and the known bond distances (Table 1) for the vanadium compounds shown in Fig. 14. The steps in the analysis are given in the following: (a) Fixing $\zeta = 2$, the free atom value for oxygen, and varying the c_1/c_2 ratio, the slope never attains or exceeds 2.0; but maximizes at 1.8 with $c_1/c_2 \sim 0.3$. (b) However, when ζ is varied at fixed c_1/c_2, the slope is found to be dependent on ζ and can have values greater or smaller than 2.0. With c_1/c_2 in the range 0.3 to 1.0, ζ varies from 1.67 to 1.75 in order to have the slope equal to 2.0. This range of ζ values (which is smaller than the free atom value) is consistent with a value of 1.7 calculated for the O^- ion.[76] (c) Finally, by using $\zeta = 1.70$ as a fixed value, the slope was found to vary monotonically

with c_1/c_2. A least-squares fit of the slope versus c_1/c_2 yields a slope of 2 at $c_1/c_2 = 1.10$. This c_1/c_2 ratio yields a 55% = $\frac{c_1^2}{c_1^2 + c_2^2} \times 100$ contribution of the short bond to the observed intensity according to Equation (6).

In Fig. 15, a self-consistent simulation with $c_1 = c_2$ is plotted for the vanadium compounds which show the pre-edge transition. The solid line having a slope of 2.05 was calculated using $\zeta = 1.7$ for all compounds including those of VPc and VTPP each of which contains four N ligands. When $\zeta = 1.6$ is used in the second term of the RHS of Equation (6) for these two compounds, we obtain the dotted line the slope of which is lower (1.97), but is within the accuracy of the simulation.

Thus, using a quantum mechanical expression of the kind given in Equation (6), one can combine a set of geometry-sensitive curves like those shown in Fig. 14 into a single curve (Fig. 15) which contains structural information in terms of bond distances as well as bonding information in terms of orbital exponents, ζ, for the appropriate ligands. Furthermore, the effect of the short V-O bond on the pre-edge intensity can also be evaluated in terms of the c_i coefficients. However, the intensity is dependent on two (or more) bond lengths in the molecular cage, thus it is not possible to use the relationship given in Equation (6) to predict the bond length.

III.H Energy Shifts and Coordination Charge

In Section III.B we saw that the energy positions (or chemical shifts[52]) of the threshold, pre-edge peak, the K-edge and the $1s \rightarrow 4p$ transition in the XANES spectra of the oxides of vanadium are related linearly to the formal valence of the central vanadium atom (see Fig. 5). This, of

course, is Kunzl's law[52] and has been shown useful for systems having the same ligand type[77-80], e.g. oxygen in the oxide series: VO, V_2O_3, V_4O_7, V_2O_4, and V_2O_5. More generally, the chemical shifts in x-ray edge spectra are due to a combination of valence, electronegativity of the bonding ligands, coordination number and other structural features. These factors may approximately be accounted for by the concept of coordination charge, η, defined by Batsanov[81] as

$$\eta = Z - CN \tag{7}$$

where Z is the formal valence of the central atom, C is the degree of covalency which equals 1 - i, i being ionicity, and N is the coordination number. For a purely ionic material like NaCl, C=0 and η=Z, i.e. valence of a constituent atom equals its coordination charge.

Now the multiple-bond ionicity i is given by

$$i = 1 - \frac{Z}{N}\exp\left[-\frac{1}{4}(X_A - X_B)^2\right] \tag{8}$$

and

$$I = 1-\exp\left[-\frac{1}{4}(X_A - X_B)^2\right] \tag{9}$$

is the single bond ionicity.[82] Combining Equations (7), (8), and (9), we obtain

$$\eta = ZI \tag{10}$$

which is the charge appearing at the periphery of the atom as a result of chemical bonding to its ligands. In qualitative terms, the coordination charge concept simply states that as the valence electrons are pulled away from the metal atom by the electronegativity, X_B, of the coordinating ligands, all of the other electrons of the central atom become more tightly bound in

order to shield the unchanging nuclear charge. Hence a K-shell transition must increase in energy with an increase in the product of valence Z and ionicity, I. The coordination charge concept has been used by Cramer et al.[12] to identify the chemical state of Mo in nitrogenase from chemical shift data of a series of Mo model compounds. More recently Lytle et al.[20a] have correlated the intensity of the L_{111}-white line in some Au, Pt and Ir compounds with coordination charge on the metal atoms.

In Table 3, the pertinent quantities are listed and the coordination charge calculated for a variety of vanadium formal valences and ligands relevant to this investigation. In cases where the first coordination shell is mixed, a weighted average electronegativity was used. In Fig. 16, the energy positions of the absorption threshold as determined by the first peak in the derivative spectra (Fig. 2a, 4, 7, 9, 11, and 13) and the main absorption edge (Table 2) for all the vanadium compounds studied here are plotted versus coordination charge. Although there is considerable scatter, particularly for the main absorption edge where a variety of spectral features occurring in the edge make identification of the edge rather subjective, the simple coordination charge concept allows a much more systematic and general organization of the data than valence alone. In compounds such as VH, VB_2, VSi_2, VP, and VC, the bonding is essentially metallic in nature. The coordination charge of the vanadium center in these intermetallic compounds is low, and yields lower threshold and K-edge energies compared with the more strongly, chemically bonded oxides and oxy-compounds. Ligand electronegativity effects can be seen in the cases of V_2S_3 versus V_2O_3, and the nitrogen-containing VPc and VTPP versus VOPBD and V_2O_4. For compounds that exhibit a pre-edge absorption, the energy position of this feature is plotted versus in Fig. 17. The

lines in both Figs. 16 and 17 were drawn using linear regression analysis and have slopes equal to 3.4, 1.4, and .9 eV per coordination charge unit for the K-edge, the threshold, and pre-edge peak respectively. The differences in slopes are statistically significant. They are also chemically reasonable in that the pre-edge peak (with final states primarily of the V 3d character) is at lower energy and is expected to be more tightly bound, hence less sensitive to changes in valence and ionicity than the more diffuse, higher energy 4s and 4p final states. In general terms, the well defined 3d level is "hard". The ns and np continuum are "softer".

IV. Concluding Remarks

With intense and well-collimated synchrotron radiation as a light source, high resolution spectral features in the vicinity of the x-ray absorption edges not previously recorded with conventional x-ray tube sources can now be obtained routinely and with good accuracy. The existence of a wide range of chemical structures in vanadium compounds greatly facilitates a systematic study of the effect of valence, site symmetry, coordination geometry, ligand electronegativity, and bond distances on various absorption features in the XANES spectra of a single constituent atom.

Particularly informative is the pre-edge absorption in the V K-edge spectra of these compounds. Its occurrence, energy position and intensity can now be understood in terms of site symmetry, coordination charge on the x-ray absorbing V atom, bond distances, and electronegativity of the coordinating ligands. In perfect octahedral symmetry which has a center of inversion, the $1s \rightarrow 3d$ transition is only quadrupole-allowed and thus is very weak. Progressively lowering the site symmetry to a distorted octahedral, square

pyramidal and tetrahedral geometries promotes the dipole-allowedness of the pre-edge absorption and yields an increasing intensity. This is due to the different mixing of metal and ligand character allowed by the change in local symmetry about the metal atom. This trend of intensity change with local site symmetry is seen clearly in the pre-edge peaks of VO, V_2O_3, V_4O_7, V_2O_5 (Fig. 3) and the vanadates (Fig. 10).

The observed intensity of the pre-edge can be related quantitatively to cage size of the metal-ligand cluster defined by the short V-O bond length and the average of the remaining longer V-ligand bonds according to $I \sim \left[c_1(\gamma R_1)^2 \exp(-\zeta \gamma R_1) + c_2(\gamma R_2)^2 \exp(-\zeta \gamma R_2)\right]^2$ as described in Section III-G. Systematic simulations lead to a self-consistent value of orbital exponent value, ζ, of 1.67-1.75 which agrees with the theoretical value of 1.70 for the O^- ions. Using a theoretical slope of 2 as a criterion of fit in the plot of ln I versus ln $\left[c_1(\gamma R_1)^2 \exp(-\zeta \gamma R_1) + c_2(\gamma R_2)^2 \exp(-\zeta \gamma R_2)\right]$ the contribution of the short bond in determining the intensity of the pre-edge peak is found to be 55%. The value is much higher than values of 16-20% that correspond to the fractions of short V-O bond to the total number of V-ligand bonds in these compounds.

In this study, the XANES spectra of VH, VB_2, VC, VN, VP, and VSi_2 are also reported. The V K-edge spectra of these intermetallics may be rather structureless as in the case of VH, or rather complex as in the case of VSi_2. The understanding of the near-edge absorption features of these intermetallics is far from being satisfactory when compared with the non-metallic oxygen and nitrogen compounds discussed in this study. Band structure effects are expected to play a role in determining the observed absorption characteristics, but calculations are not available for these vanadium intermetallic

compounds at sufficient energy above the Fermi level. In the case of VO[83] and VC[84] the band structures were calculated only to a few eV's above the Fermi level. It is our hope that further theoretical work will be simulated for this class of materials in the future, and that calculated density of state (DOS) and projected DOS will become available for energies 20-30 eV above the Fermi level.

Finally, it may be remarked that the trends observed for various spectral variables in the V K-edge XANES spectra of these compounds represent a useful data base for an improved understanding of absorption edge theory and/or for characterizing and identifying the structure and bonding of V in unknown materials.

Acknowledgements

We would like to acknowledge experimental opportunities at Stanford Synchrotron Radiation Laboratory (SSRL) which is supported by the U.S. Department of Energy. The research of FWL was supported in part by NSF and ONR.

Figure Captions

Fig. 1 Room temperature V K-edge absorption spectrum of vanadium metal showing schematically the edge normalization procedure (see text). The zero of energy is taken with respect to the first peak in the derivative spectrum shown in Fig. 2(a) at 5465 eV.

Fig. 2 (a) Derivative and (b) normalized absorption spectra of vanadium metal in the range ± 70 eV.

Fig. 3 Normalized K-edge XANES spectra of vanadium oxides, the zero of energy is taken at 5465 eV.

Fig. 4 Derivative plots of the K-edge spectra of vanadium oxides shown in Fig. 3.

Fig. 5 Oxidation state versus energy positions of various absorption features in the V K-edge XANES spectra of various vanadium oxides.

Fig. 6 Normalized V K-edge XANES spectra of roscoelite and V_2S_3.

Fig. 7 Derivative plots of the K-edge spectra of roscoelite and V_2O_3 shown in Fig. 6.

Fig. 8 Normalized V K-edge XANES spectra of a series of vanadyl compounds. VOPBD = vanadyl bis 1-phenyl 1,3 butane dionate, VTPP = vanadyl tetraphenyl porphyrin; VPc = vanadyl phthalocyanine.

Fig. 9 Derivative plots of the K-edge spectra of vanadyl compounds shown in Fig. 8.

Fig. 10 Normalized V K-edge XANES spectra of NH_4VO_3, $CrVO_4$, and vanadinite.

Fig. 11 Derivative plots of the K-edge spectra of NH_4VO_3, $CrVO_4$, and vanadinite shown in Fig. 10.

Fig. 12 Normalized V K-edge XANES spectra of a series of intermetallic compounds.

Fig. 13 Derivative plots of the K-edge spectra of the series of intermetallic compounds shown in Fig. 12. The spike above 40 eV is a glitch.

Fig. 14 Intensity of pre-edge absorption versus average bond length $\bar{R}$ of first shell ligands in various cage geometries.

Fig. 15 Plot of ln I vs. $\ln\left[(\gamma R_1)^2 e^{1.7\gamma R_1} + (\gamma R_2)^2 e^{-\zeta\gamma R_2}\right]$ using the same (solid line) and different (dotted line) values of ζ for oxygen and nitrogen compounds.

Fig. 16 Coordination charge on the V absorber vs energy positions of (a) the threshold of K photoelectron ejection, and (b) main absorption edge of V in all the vanadium compounds studied here.

Fig. 17 Coordination charge on the vanadium absorber versus energy position of pre-edge absorption in some vanadium compounds.

References

1. M. C. Srivastava and H. L. Nigam, Coordin. Chem. Rev. 9 275 (1972).

2. L. V. Azaroff and D. M. Pease, in X-ray Spectroscopy (L. V. Azaroff, ed.) McGraw Hill, New York (1974) Chap. 6.

3. E. W. White and H. A. McKinstry, Adv. X-ray Analysis 9, 376 (1966).

4. P. E. Best, J. Chem. Phys. 44, 3248 (1966).

5. W. Seka and H. P. Hanson, J. Chem. Phys. 50, 344 (1969).

6. D. W. Fischer, J. Appl. Phys. 41, 3561 (1970).

7. K. Tsutsumi, O. Aita, and K. Ichikawa, Phys. Rev. B10, 4638 (1977).

8. D. W. Fischer and W. L. Baun, J. Appl. Phys. 39, 4757 (1968).

9. L. F. Mattheis, Phys. Rev. 134, A970 (1964).

10. V. Ern and A. C. Switendick, Phys. Rev. 137, A1927 (1965).

11. R. G. Shulman, Y. Yafet, P. Eisenberger, W. E. Blumberg, Proc. Nat. Acad. Sci. USA 73, 1384 (1976).

12. S. P. Cramer, T. K. Eccles, F. W. Kutzler, K. O. Hodgson, L. E. Mortenson, J. Am. Chem. Soc. 98, 1287 (1976).

13. V. O. Kostroun, R. W. Fairchild, C. A. Kukkonen, J. W. Wilkins, Phys. Rev. B13 3268 (1976).

14. V. W. Hu, S. I. Chan, and G. S. Brown, Proc. Nat. Acad. Sci. USA, 74, 3821 (1977).

15. J. E. Miller, O. Jepsen, O. K. Anderson, J. W. Wilkins, Phys. Rev. Lett. 40, 720 (1978).

16. S. P. Cramer, K. O. Hodgson, E. I. Stiefel, W. E. Newton, J. Amer. Chem. Soc. 100, 2748 (1978).

17. M. Belli, A. Scafati, A. Bianconi, S. Mobilio, L. Palladino, A. Reale, and E. Burattini, Solid State Comm. 35, 355 (1980).

18. R. B. Greegor, F. W. Lytle, D. R. Sandstrom, J. Wong, and P. Schultz, J. Non-Crystalline Solids 55, 27 (1983).

18a. L. A. Grunes, Phys. Rev. B27, 2111 (1983).

19. C. L. Spiro, J. Wong, F. W. Lytle, R. B. Greegor, D. Maylotte, and S. Lamson, Science (submitted)

20. P. S. P. Wei and F. W. Lytle, Phys. Rev. B19, 679 (1979).

20a. F. W. Lytle, P. S. P. Wei, R. B. Greegor, G. H. Via, and J. H. Sinfelt, J. Chem. Phys. 70, 4849 (1979).

21. K. J. Rao, J. Wong, and M. J. Weber, J. Chem. Phys. 78, 6228 (1983).

22. K. J. Rao and J. Wong, Inorg. Chem. (submitted).

23. M. Brown, R. E. Peierls, and E. A. Stern, Phys. Rev. B15, 738 (1977).

24. D. H. Templeton and L. K. Templeton, Acta Cryst. A36, 237 (1980).

25. F. W. Kutzler, R. A. Scott, J. M. Berg, K. O. Hodgson, S. Doniach, S. P. Cramer, and C. H. Chang, J. Amer. Chem. Soc. 103, 6083 (1981).

26. R. J. H. Clark in Comprehensive Inorganic Chemistry, (J. C. Bailar et al., Ed.) Pergamon Press, Oxford (1973) Vol. 3 Chap. 34.

27. E. E. Vainshtein, E. A. Zhurakovskii, V. S. Nesphor, and G. V. Samsonov, Sov. Phys. (Engl. Translation) 5, 996 (1961).

28. S. I. Salem, C. N. Chang, and T. J. Nash, Phys. Rev. B18, 5168 (1978).

29. D. W. Fischer, J. Appl. Phys. 40, 4151 (1969).

30. This acronym was coined by A. Bianconi, Appl. of Sur. Sci. 6, 392 (1980).

31. T. D. Tullius, W. O. Gillum, R. M. K. Carlson, and K. O. Hodgson, J. Amer. Chem. Soc. 102, 5670 (1980).

32. D. H. Maylotte, J. Wong, R. L. St. Peters, F. W. Lytle, and R. B. Greegor, Science 214, 554 (1981).

33. J. Wong, F. W. Lytle, D. H. Maylotte, G. H. Via, Fuel (to be published).

34. A Trademark of the DuPont Company.

35. J. Wong, Nucl. Instrum. Methods (sumbitted)

36. J. A. Bearden and A. F. Burr, Rev. Mod. Phys. 39, 125 (1967).

37. J. Jaklevic, J. A. Kirby, M. P. Klein, A. S. Robertson, G. S. Brown, and P. Eisenberger, Solid State Comm. 23, 679 (1977).

38. F. W. Lytle, R. B. Greegor, D. R. Sandstrom, E. C. Marques, J. Wong, C. L. Spiro, G. P. Huffman, and F. E. Huggins, Nucl. Instrum. Methods (in press) 1984.

38(a). J. B. Pendry, in "EXAFS and Near-Edge Structure" Ed. by A. Bianconi, L. Incoccia, and S. Stipcich, Springer Series in Chemical Physics,

Vol. 27, Springer-Verlag, New York (1983) pp. 4-10.

39. J. Stringer, J. Less-Common. Metals 8, 1 (1965).

40. N. Schonberg, Acta Chem. Scand. 8, 221 (1954).

41. R. E. Newnham and Y. M. de Haan, Z. Krist. 117, 235 (1962).

42. M. Marezio, D. B. McWhan, P. D. Dernier, and J. P. Remeika, J. Solid State Chemistry 6, 419 (1973).

43. G. Anderson, Acta Chem. Scand. 10, 623 (1956); F. Thesbald, R. Cabala, and J. Bernard, J. Solid State Chem. 17, 431 (1976).

44. H. G. Bachmann, F. R. Ahmed, and W. H. Barnes, Z. Krist. 115, 110 (1961).

45. J. L. Dehmer, J. Chem. Phys. 56, 4496 (1972).

46. D. Dill and J. L. Dehmer, J. Chem. Phys. 61, 692 (1974).

47. J. L. Dehmer and D. Dill, J. Chem. Phys. 65, 5327 (1976).

48. P. J. Durham, J. B. Pandry, and C. H. Hodges, Solid State Comm. 38, 159 (1981).

49. G. N. Greaves, P. J. Durham, G. Diakun, and P. Quinn, Nature 294, 139 (1981).

50. F. W. Kutzler, C. R. Natoli, D. K. Misemer, S. Doniach, and K. O. Hodgson, J. Chem. Phys. 73, 3274 (1980).

51. V. Kunzl, Collect. Trav. Chim. Techecolovaquie 4, 213 (1932); cited in Ref. 51.

52. C. Mande and V. B. Sapre, in "Advances in X-ray Spectroscopy", Ed. C. Bonnelle and C. Mande, Pergamon Press (1983) Chap. 17, p. 287-301.

53. E. W. Heinrich and A. A. Levinson, Am. J. Sc. 253, 39 (1955).

54. F. Hullinger, Structure and Bonding 4, 83 (1968).

55. D. Tudo, Rev. Chim. Minerale 2, 153 (1965).

56. P.-K. Hon, R. L. Belford, and C. E. Pfluger, J. Chem. Phys. 43, 1323 (1965).

57. R. C. Pettersen, Acta Cryst. B25, 2527 (1969).

58. F. S. Molinaro and J. Albers, Inorg. Chem. 15, 2278 (1976).

59. R. F. Ziolo, C. H. Griffiths, and J. M. Troup, J. Chem. Soc., Dalton Trans. 2300 (1980).

60. P. F. Theobald and J. Galy, Acta Cryst. B29, 2732 (1973).

61. H. T. Evans,Jr., Z. Krist 114, 257 (1960).

62. R. W. G. Wychoff, "Crystal Structures" Wiley Interscience, 2nd Edition. Vol. 3 (1965) p. 37.

63. K. Brandt, Arkiv Kemi, Mineral. Geol. 17A No. 6 (1943).

64. F. W. Lytle, Acta Cryst. 22, 221 (1967).

65. A. F. Wells, "Structural Inorganic Chemistry" Oxford. Clarendon Press, 3rd Edition (1962) p. 183.

66. W. E. Baker, Am. Mineral 51, 1712 (1966).

67. W. Rostoker, "The Metallurgy of Vanadium" Wiley, New York (1958).

68. A. J. Maeland, J. Phys. Chem. 68(8), 2197 (1964), and reference cited therein.

69. B. Post, F. W. Glaser, and D. Moskowitz, Acta. Metal. 2, 20 (1954).

70. E. Rudy, F. Benesovsky, and L. Toth, Z. Metal 54, 345 (1963).

71. R. W. G. Wyckoff, "Crystal Structures", Wiley, 2nd Ed., Vol. 1 (1963) p. 91.

72. N. Schonberg, Acta. Chem. Scand. 8, 226 (1954).

73. V. A. Gubanov, B. G. Kasimov, and E. Z. Kurmaev, J. Phys. Chem. Solids, 36, 861 (1975).

74. H. J. Wallbaum, Z. Metall. 33, 378 (1941).

75. A. C. Wahl, P. E. Cade, and C. C. Roothaan, J. Chem. Phys. 41, 2578 (1964), Equation (III.12).

76. L. C. Cusachs and J. H. Corrington, in "Sigma Molecular Orbital Theory", Yale University Press, New Haven (1970), p. 257.

77. W. H. Zinn, Phys. Rev. 46, 659 (1930).

78. V. P. Barton, Phys. Rev. 71, 406 (1947).

79. I. Manescu, C. R. Acad. Sci. 255, 537 (1947).

80. G. L. Glenn and C. G. Dodd, J. Appl. Phys. 39, 5372 (1968).

81. S. S. Batsanov, "Electronegativity of Elements and Chemical Bonds" Novosibrsk, (1962), cited in I. A. Ovsyannikova, S. S. Batsanov, L. I. Nasonova, L. R. Batsanova, and E. A. Nekrasova, Bull. Acad. Sci. USSR, Phys. Ser. 31, 936 (1967) (English translation).

82. L. Pauling, "The Nature of the Chemical Bond", 3rd Ed., Cornell University, Ithaca (1960) p. 98.

83. T. E. Norwood and J. L. Fry, Phys. Rev. B2, 472 (1970).

84. J. Zbasnik and L. E. Toth, Phys. Rev. B8, 452 (1973).

Table 1
Relevant Structural Parameters of Vanadium Compounds

Compound	Formal Valence	Bond Type	No. of Bonds, (N)	Bond Distance (Å)	Ref.
V metal	0	V-V	8	2.622	26
VO	2	V-O	6	2.05	40
V_2O_3	3	V-O	3	1.96	41
			3	2.06	
V_4O_7	3,4	V-O	6	1.883 1.897 1.937 2.032 2.042 2.101	42
V_2O_4	4	V-O	6	1.76 1.86 1.87 2.01 2.03 2.05	43
V_2O_5	5	V-O	5	1.585 1.780 1.878 1.878 2.021	44
V_2S_3	3	V-S	6	2.08 (AV.) N,R by EXAFS	54
Roscoelite	3	V-O	6	~ 2.0	53
VOPBD	4	V-O	5	1.612 1.946 1.952 1.986 1.982	56
$VOSO_4 \cdot 3H_2O$	4	V-O	1	1.56	60
		$V-OSO_3$	2	2.02	
		$V-OH_2$	2	2.05 2.08	
VPc	4	V-O	1	1.58	59
		V-N	4	2.008 2.024 2.034 2.038	
VTPP	4	V-O	1	1.62	57 58
		V-N	4	2.097 2.099 2.102 2.110	
NH_4VO_3	5	V-O	4	1.66 1.66 1.81 1.81	61
$CrVO_4$	5	V-O	4	1.72 1.72 1.80 1.80	62 63
$Pb_5(VO_4)_3^4Cl$	5	V-O	4	~ 1.75	65 66
VH	1	V-H	6		68
VB_2	4	V-B	12	2.31	69
VC	4	V-C	6	2.091	70
VN	3	V-N	6	2.07	71
VP	3	V-P	6	2.41	72
VSi_2	4	V-Si	6	2.50	74
			6	2.64	

Note: Roscoelite is $KAlV_2Si_3O_{10}(OH)_2$; VOPBD is vanadyl bis 1-phenyl-1,3 butane dionate; VPc is vanadyl phthalocyanine; VTPP is vanadyl tetraphenyl porphyrin.

Table 2

Energy Positions of Various Spectral Features in the V K-edge XANES Spectra of Vanadium Compounds, ± 0.2 eV

Compound	Threshold	Pre-Edge Peak	Main Edge	1s → 4p Transition
V Metal	0	10	8.8	19.3
VO	.8	—	8	20.4
V_2O_3	1.9	3.4	10.7	23.5
V_4O_7	2.1	4.1	11.8	25.1
V_2O_4	3.5	4.5	14	26.2
V_2O_5	4.8	5.6	15.1	30.1
HH_4VO_3	4.1	4.8	17.2	26.6
$CrVO_4$	4.1	4.8	17.6	24.2
Vanadanite	3.9	4.5	~ 18	25.1
V_2S_3	.6		10.5	23.5
Roscoelite	1.9	2.6	10.6	21.5
VOPBD	3.5	4.1	14.9	19.8
VPc	3.0	3.9	13.4	27.3
VTPP	3.5	4.1	13.4	25.7
$VOSO_4 \cdot 3H_2O$	4.1	4.8	15.6	21.0
VH	.61	—	6	18.7
VB_2	1.2	—	7.9	19.1
VC	1.5	5.4	9.9	20.4
VN	1.5	4.8	8.7	19.8
VP	1.5	4.8(sh)	7	20.
VSi_2	.5	—	7.9	27.7

Table 3

Spectral Characteristics of Pre-Edge Peak
in Vanadium Compounds

Compound	Energy Position (±0.2 eV)	Peak Height (±0.02)	Half Width, $\nu_{1/2}$ (±0.2 eV)	Intensity Height x $\nu_{1/2}$
V_2O_3	3.4	0.06	~ 7	~ 0.4
V_4O_7	4.1	.19	5.1	.97
V_2O_4	4.5	.35	4.1	1.43
V_2O_5	5.6	.79	3.15	2.48
VOPBD	4.1	.61	2.38	1.45
$VOSO_4 \cdot 3H_2O$	4.1	.48	2.04	.98
VPc	3.9	.79	2.63	2.09
VTPP	4.1	.57	2.29	1.31
NH_4VO_3	4.8	.91	2.55	2.32
$CrVO_4$	4.8	.82	2.30	1.89
$Pb_5(VO_4)_3Cl$	4.5	1.06	1.96	2.07

Table 4

Calculation of Coordination Charge

Element	Pauling Electronegativity, X [a]	Vanadium Bond Ionicity I	Bond Type	Coordination Charge η
V	1.63	0 (by definition)	V-V	0
O	3.44	0.56	V^{+2}-O	1.12
			V^{+3}-O	1.68
			$V^{+3.5}$-O	1.95
			V^{+4}-O	2.24
			V^{+5}-O	2.80
N	3.04	.39	V^{+3}-N	1.17
			V^{+4}-N	1.56
			O-V^{+4}-N_4	1.70
S	2.58	0.20	V^{+3}-S	0.60
C	2.55	0.19	V^{+4}-C	0.76
B	2.0	.034	V^{+4}-B	1.36
P	2.19	0.075	V^{+3}-P	0.22
Si	1.90	0.018	V^{+4}-Si	0.07
H	2.20	0.078	V^{+1}-H	0.08

(a) From F. A. Cotton and G. Wilkinson, "Advanced Inorganic Chemistry", 2nd Edition, Interscience (1972) p. 15.

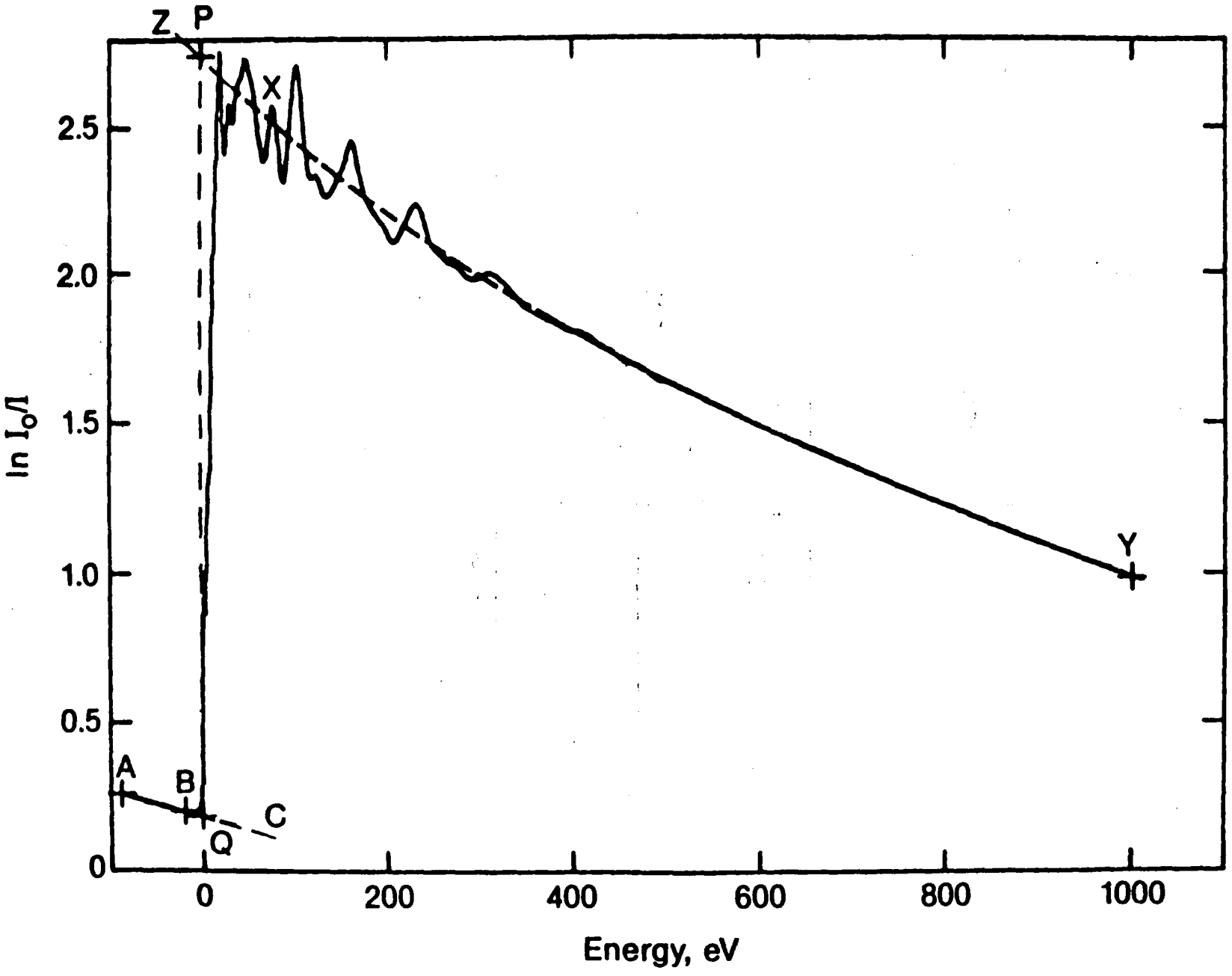

Fig. 1

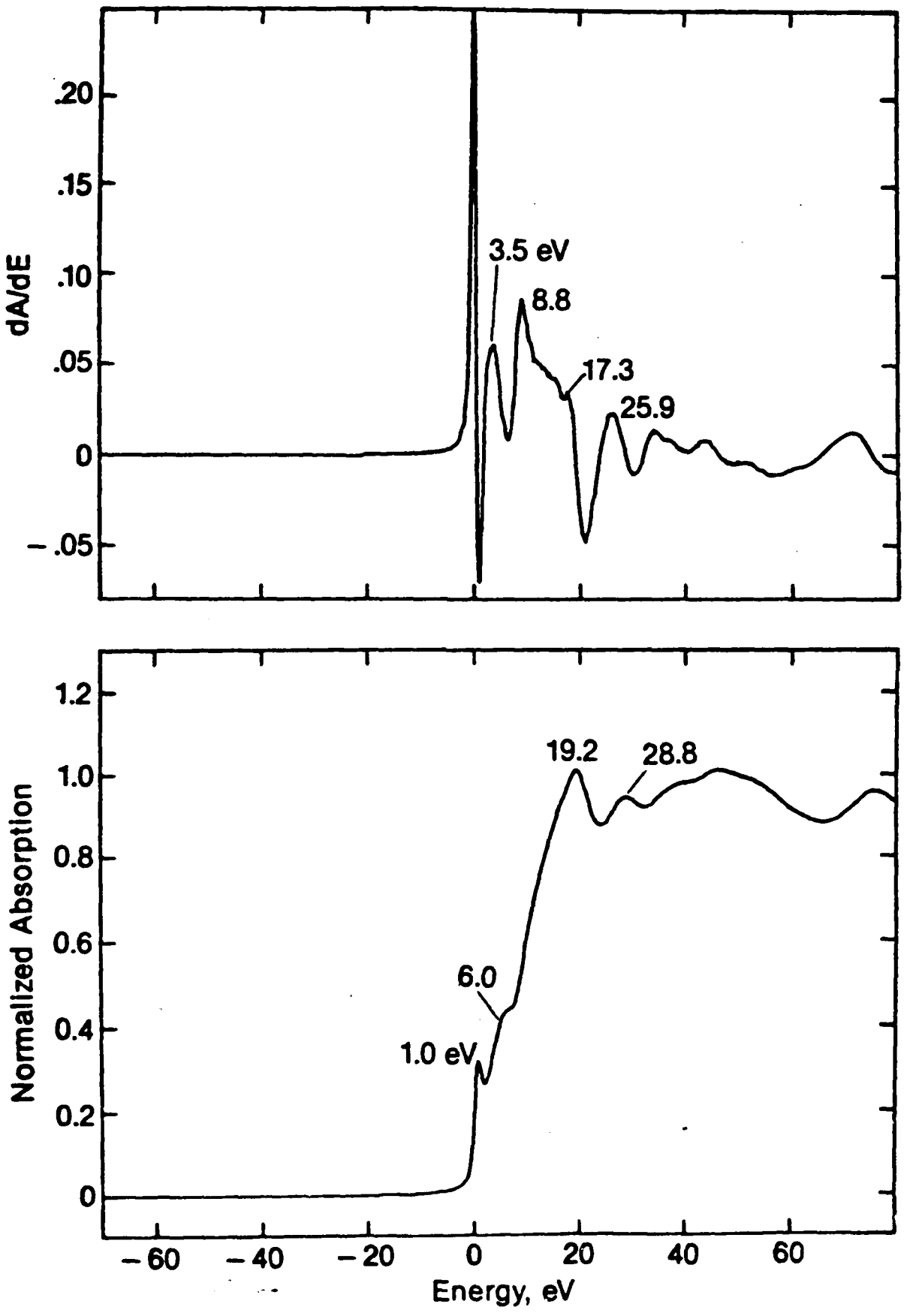
dA/dE
.20
.15
.10
.05
0
-.05
3.5 eV
8.8
17.3
25.9
Normalized Absorption
1.2
1.0
0.8
0.6
0.4
0.2
0
19.2
28.8
6.0
1.0 eV
-60
-40
-20
0
20
40
60
Energy, eV

Fig. 2

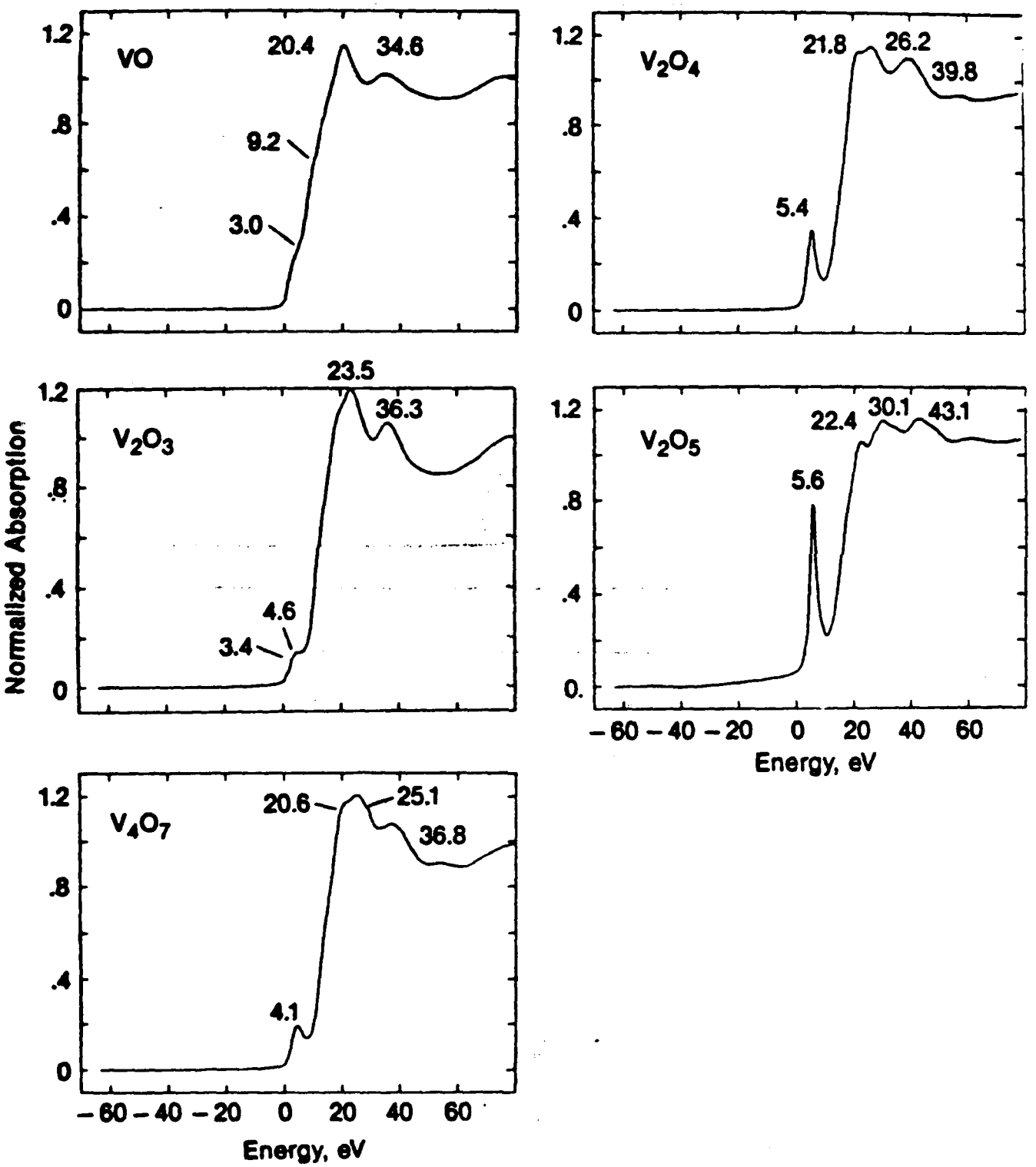
VO
20.4
34.6
9.2
3.0
V_2O_4
21.8
26.2
39.8
5.4
V_2O_3
23.5
36.3
4.6
3.4
V_2O_5
22.4
30.1
43.1
5.6
V_4O_7
20.6
25.1
36.8
4.1
Normalized Absorption
1.2
.8
.4
0
0.
−60 −40 −20 0 20 40 60
Energy, eV

Fig. 3

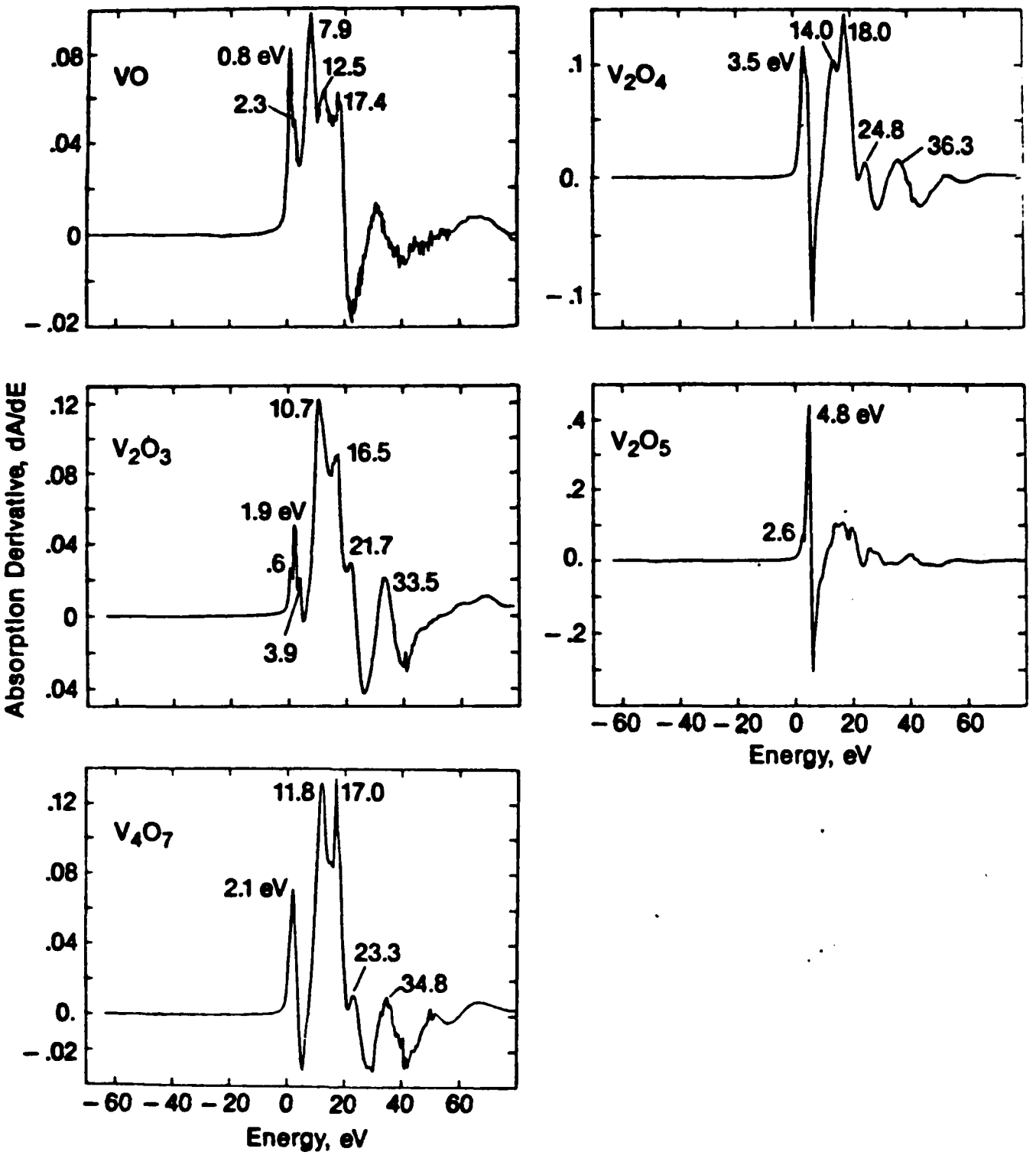
VO
0.8 eV
2.3
7.9
12.5
17.4
.08
.04
0
-.02
V_2O_4
3.5 eV
14.0
18.0
24.8
36.3
.1
0.
-.1
V_2O_3
1.9 eV
.6
3.9
10.7
16.5
21.7
33.5
.12
.08
.04
0
.04
V_2O_5
2.6
4.8 eV
.4
.2
0.
-.2
V_4O_7
2.1 eV
11.8
17.0
23.3
34.8
.12
.08
.04
0.
-.02
-60 -40 -20 0 20 40 60
Energy, eV
Absorption Derivative, dA/dE

Fig 4

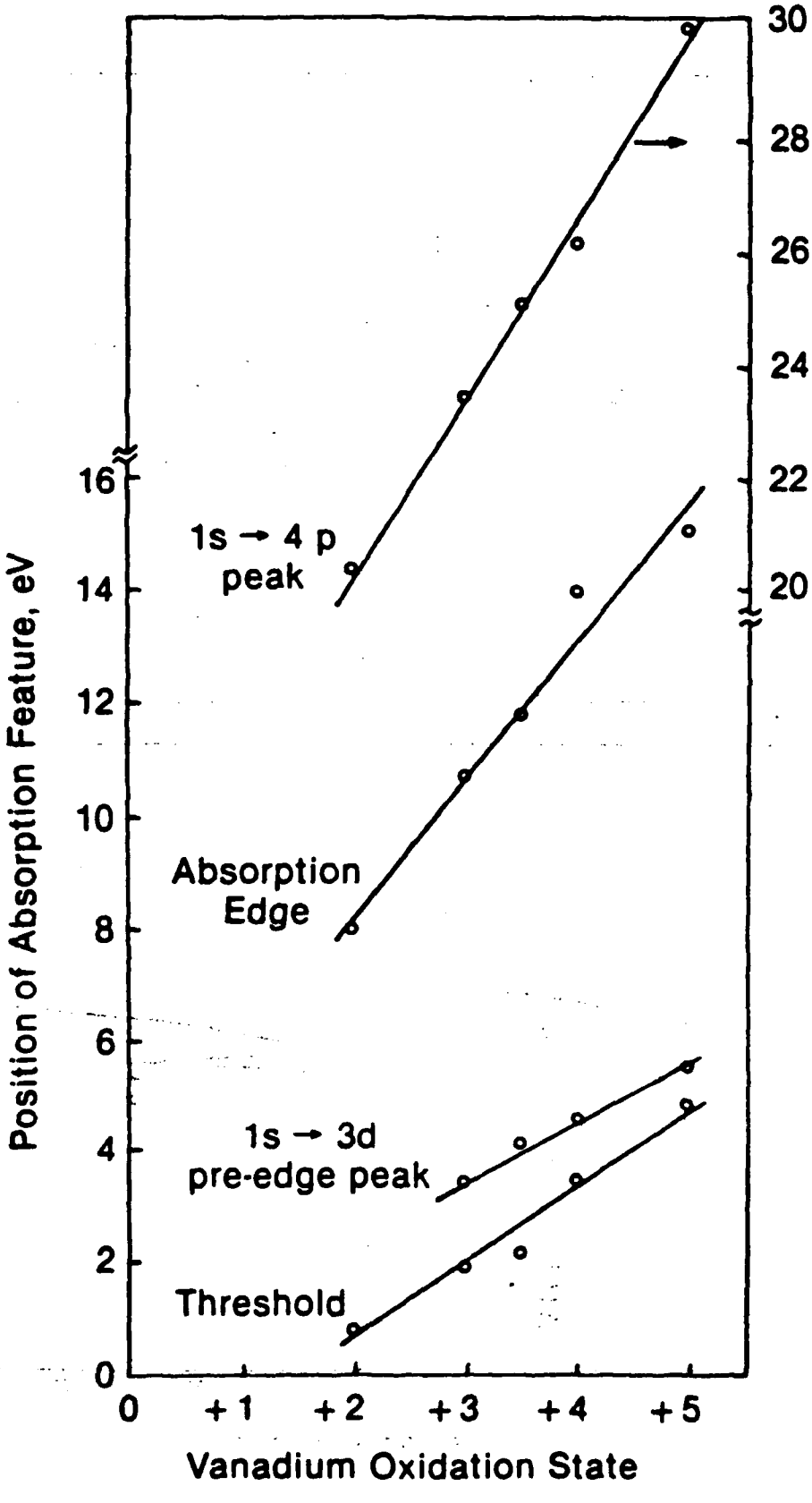
Position of Absorption Feature, eV
Vanadium Oxidation State
1s → 4 p peak
Absorption Edge
1s → 3d pre-edge peak
Threshold
0
2
4
6
8
10
12
14
16
20
22
24
26
28
30
0
+1
+2
+3
+4
+5

Fig. 5

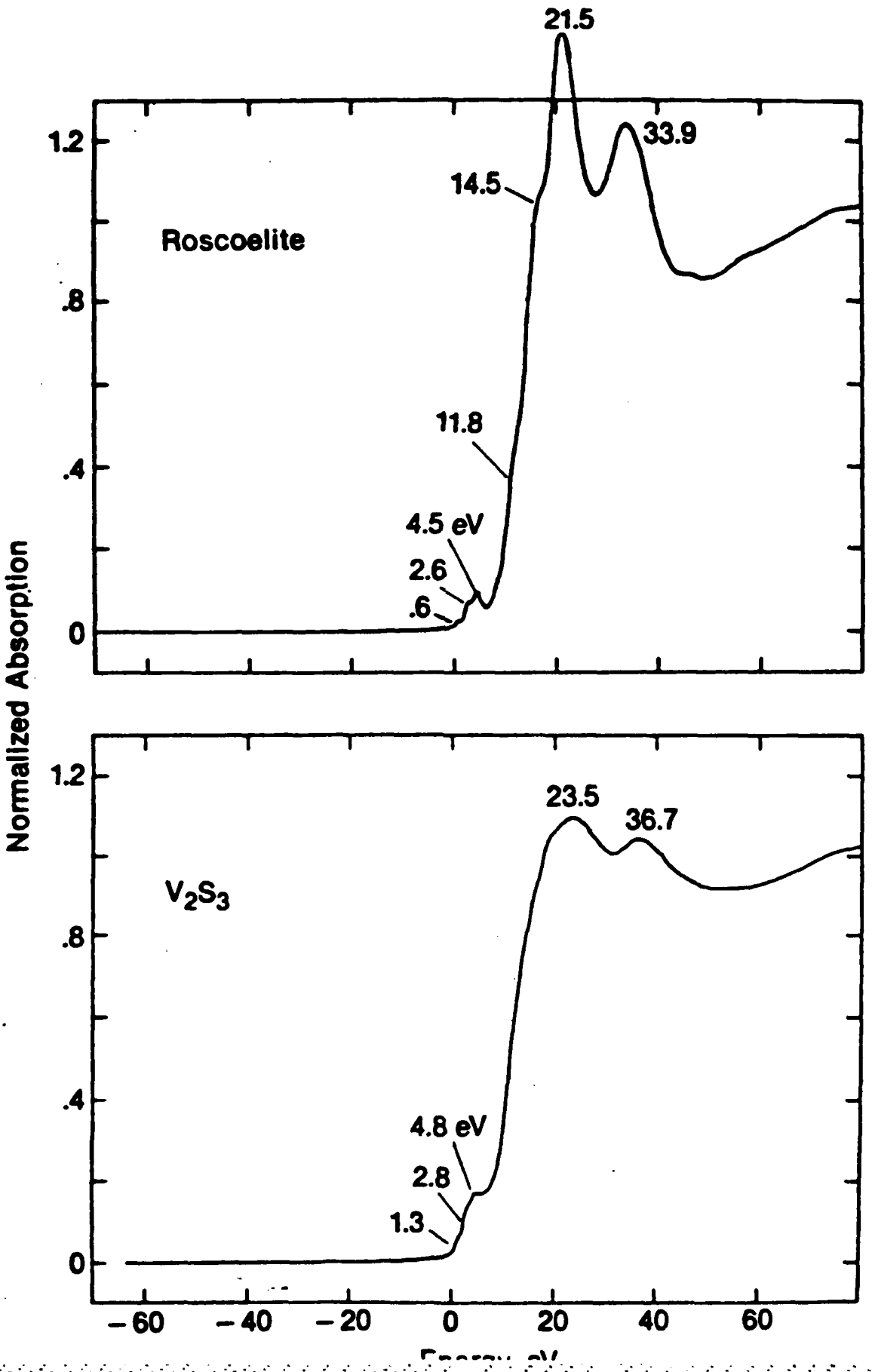
21.5
33.9
14.5
Roscoelite
11.8
4.5 eV
2.6
.6
1.2
.8
.4
0
Normalized Absorption
23.5
36.7
V_2S_3
4.8 eV
2.8
1.3
1.2
.8
.4
0
−60
−40
−20
0
20
40
60

Fig. 6

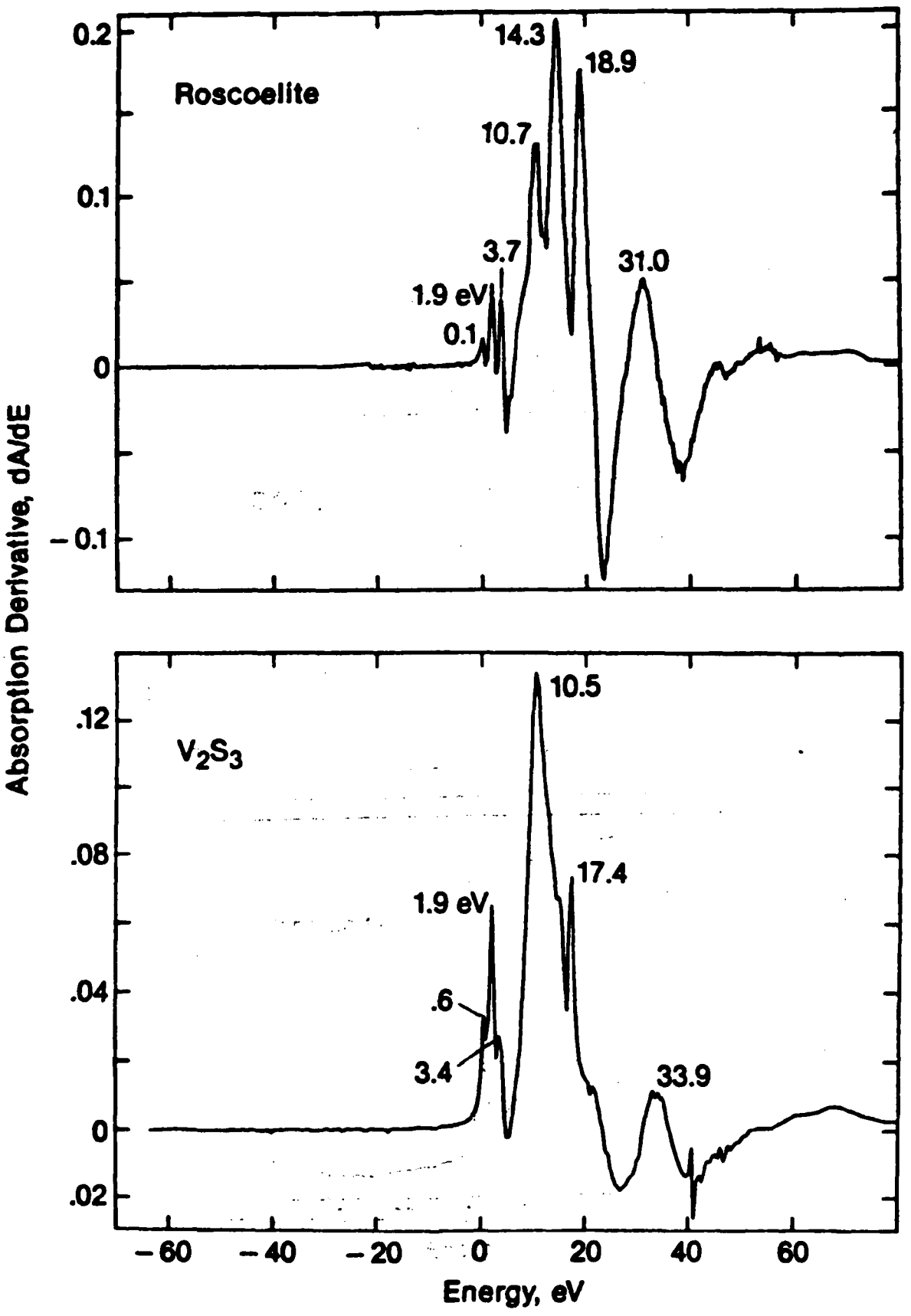
Roscoelite
14.3
18.9
10.7
3.7
31.0
1.9 eV
0.1
0.2
0.1
0
−0.1
V_2S_3
10.5
17.4
1.9 eV
.6
3.4
33.9
.12
.08
.04
0
.02
−60
−40
−20
0
20
40
60
Energy, eV
Absorption Derivative, dA/dE

Fig. 1

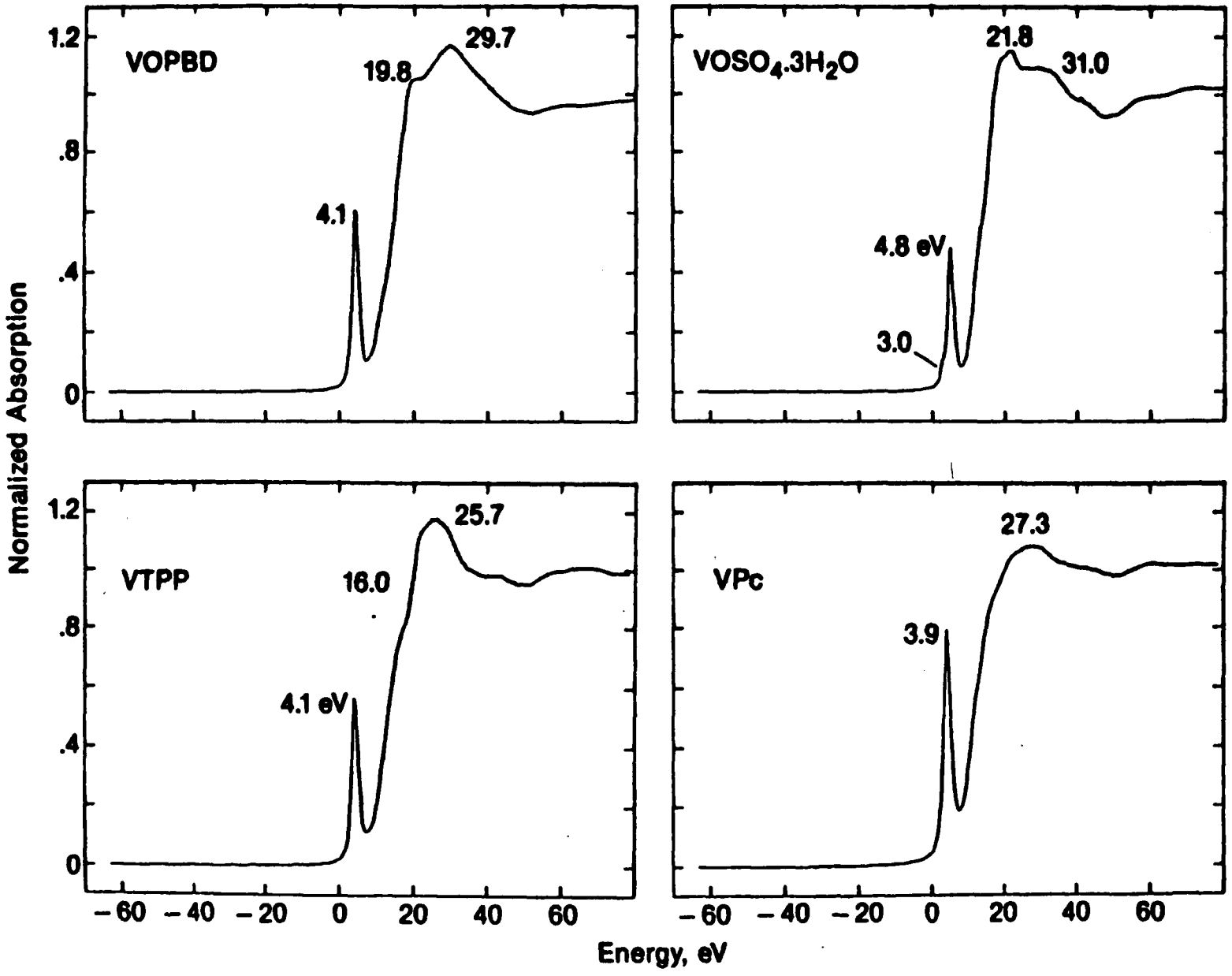
VOPBD
1.2
.8
.4
0
4.1
19.8
29.7
VOSO4.3H2O
21.8
31.0
4.8 eV
3.0
VTPP
25.7
16.0
4.1 eV
VPc
27.3
3.9
Normalized Absorption
−60 −40 −20 0 20 40 60
Energy, eV

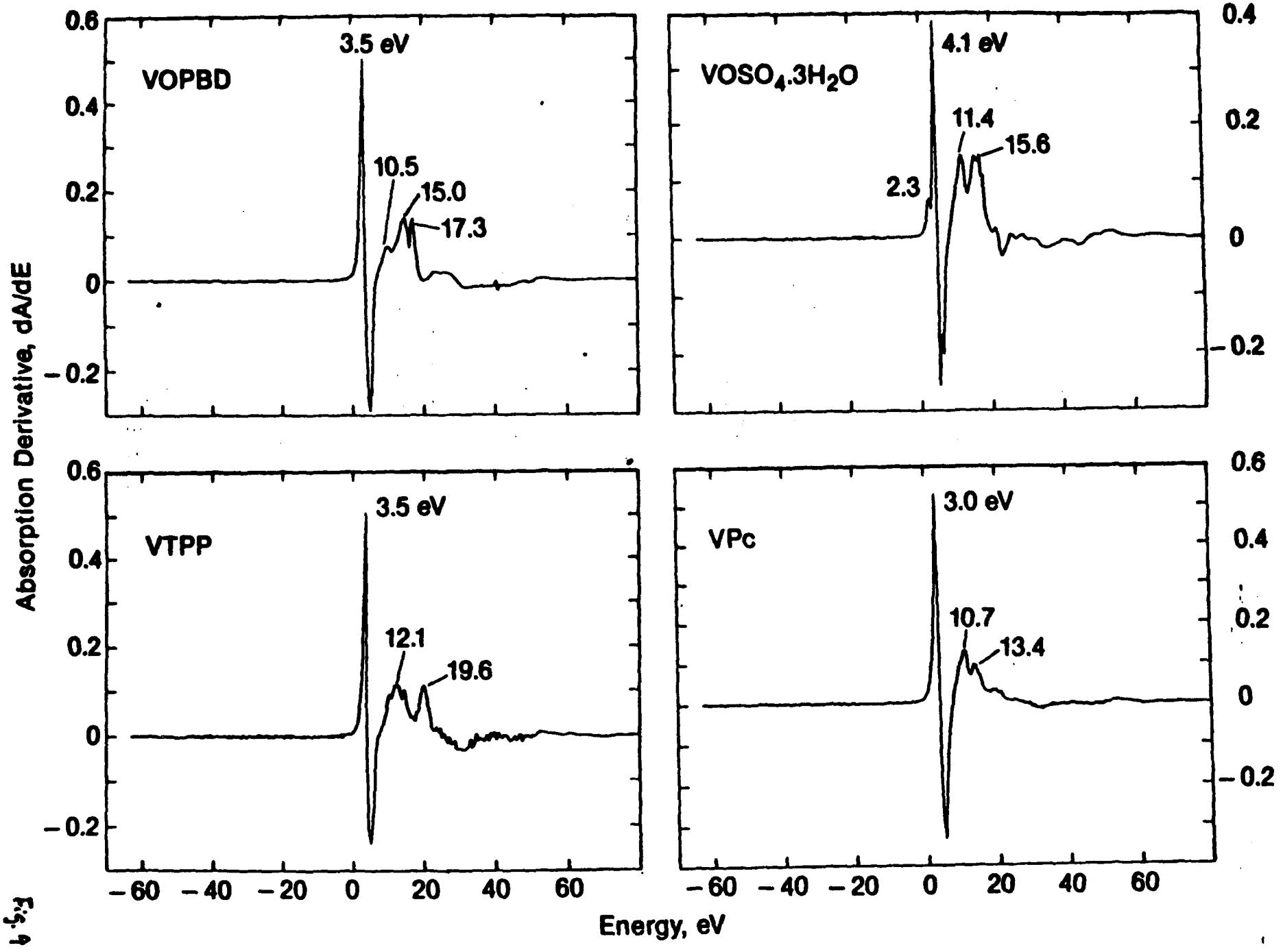
VOPBD
3.5 eV
10.5
15.0
17.3
$VOSO_4.3H_2O$
4.1 eV
2.3
11.4
15.6
VTPP
3.5 eV
12.1
19.6
VPc
3.0 eV
10.7
13.4
Absorption Derivative, dA/dE
Energy, eV
0.6
0.4
0.2
0
−0.2
−60
−40
−20
20
40
60

Fig. 4

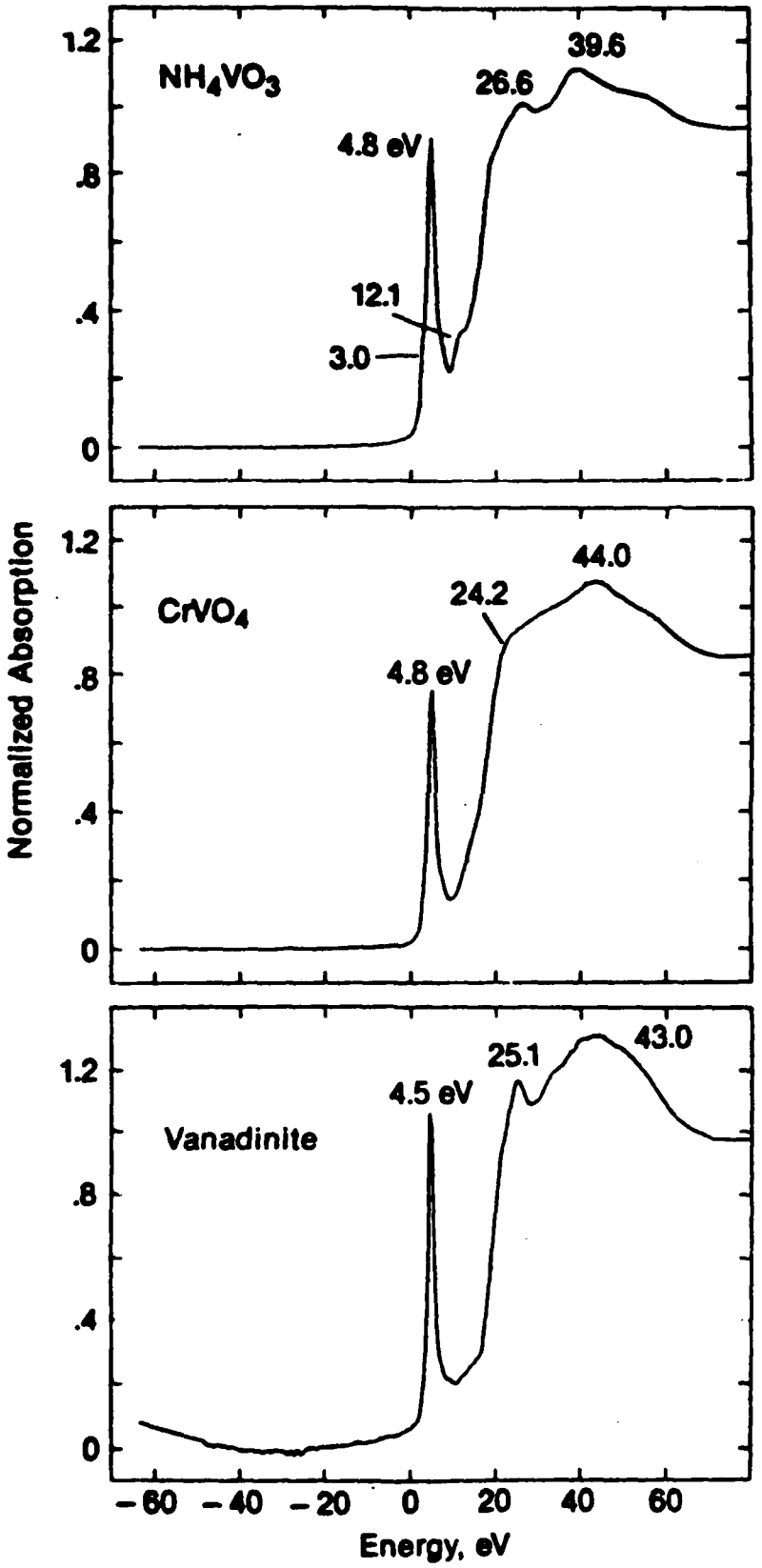
1.2
.8
.4
0
NH_4VO_3
39.6
26.6
4.8 eV
12.1
3.0
$CrVO_4$
44.0
24.2
4.8 eV
Vanadinite
25.1
43.0
4.5 eV
Normalized Absorption
−60 −40 −20 0 20 40 60
Energy, eV

Fig. 10

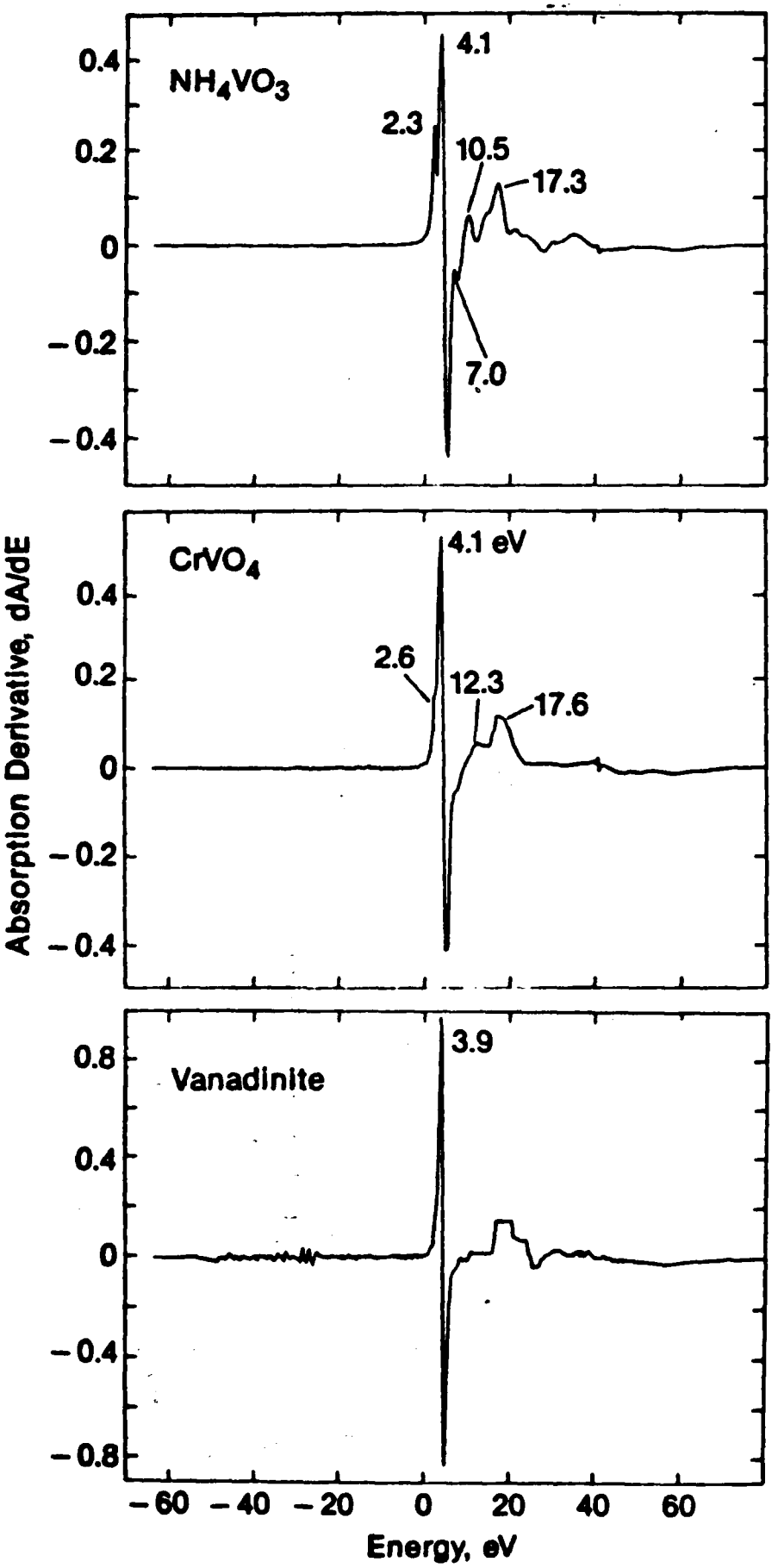
NH_4VO_3
4.1
2.3
10.5
17.3
7.0
$CrVO_4$
4.1 eV
2.6
12.3
17.6
Vanadinite
3.9
0.4
0.2
0
−0.2
−0.4
0.8
−0.8
−60
−40
−20
20
40
60
Absorption Derivative, dA/dE
Energy, eV

Fig. 1

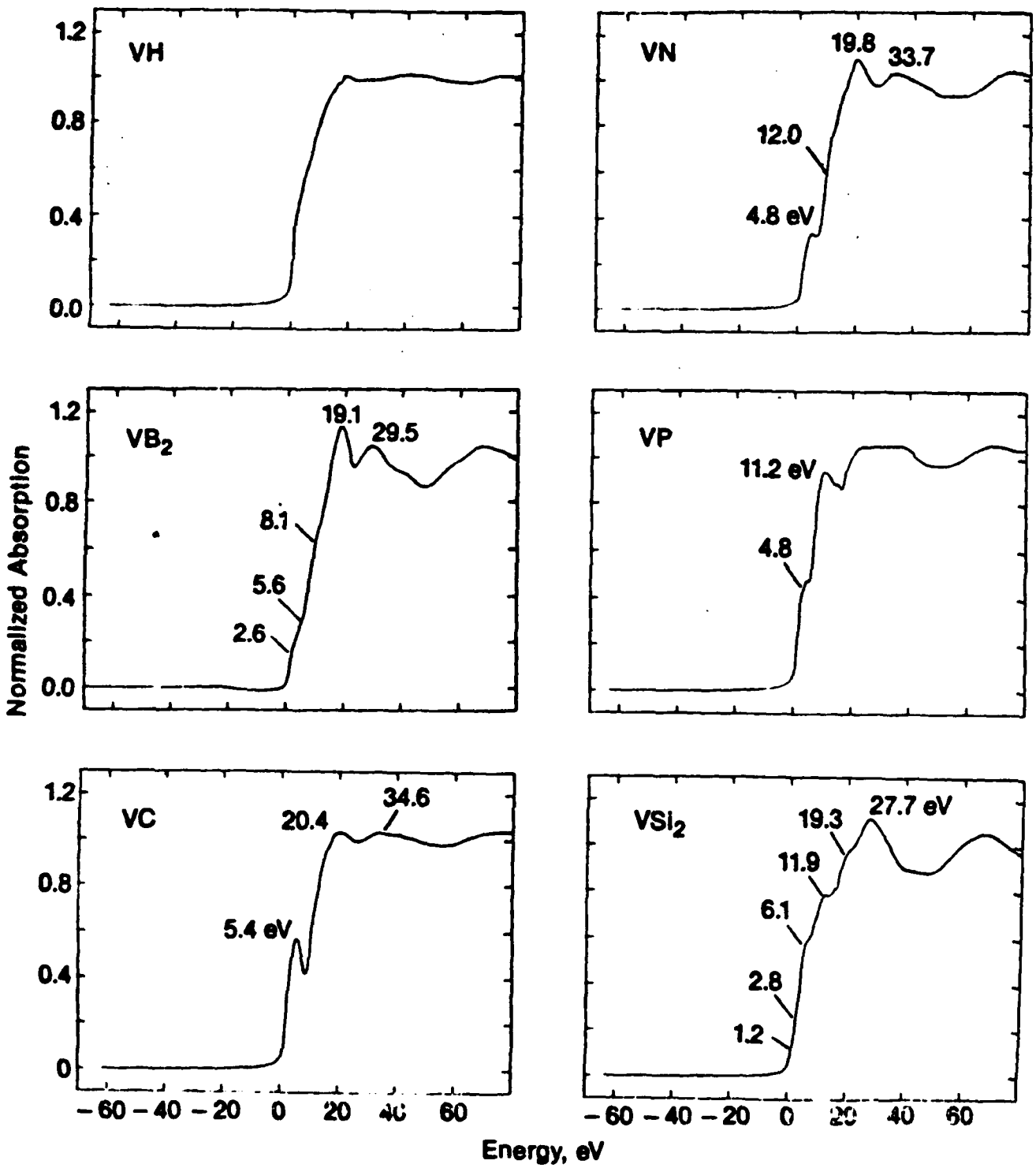
VH
VN
19.8
33.7
12.0
4.8 eV
VB2
19.1
29.5
8.1
5.6
2.6
VP
11.2 eV
4.8
VC
20.4
34.6
5.4 eV
VSi2
19.3
27.7 eV
11.9
6.1
2.8
1.2
Normalized Absorption
0.0
0.4
0.8
1.2
0
−60 −40 −20 0 20 40 60
Energy, eV

Fig. 12

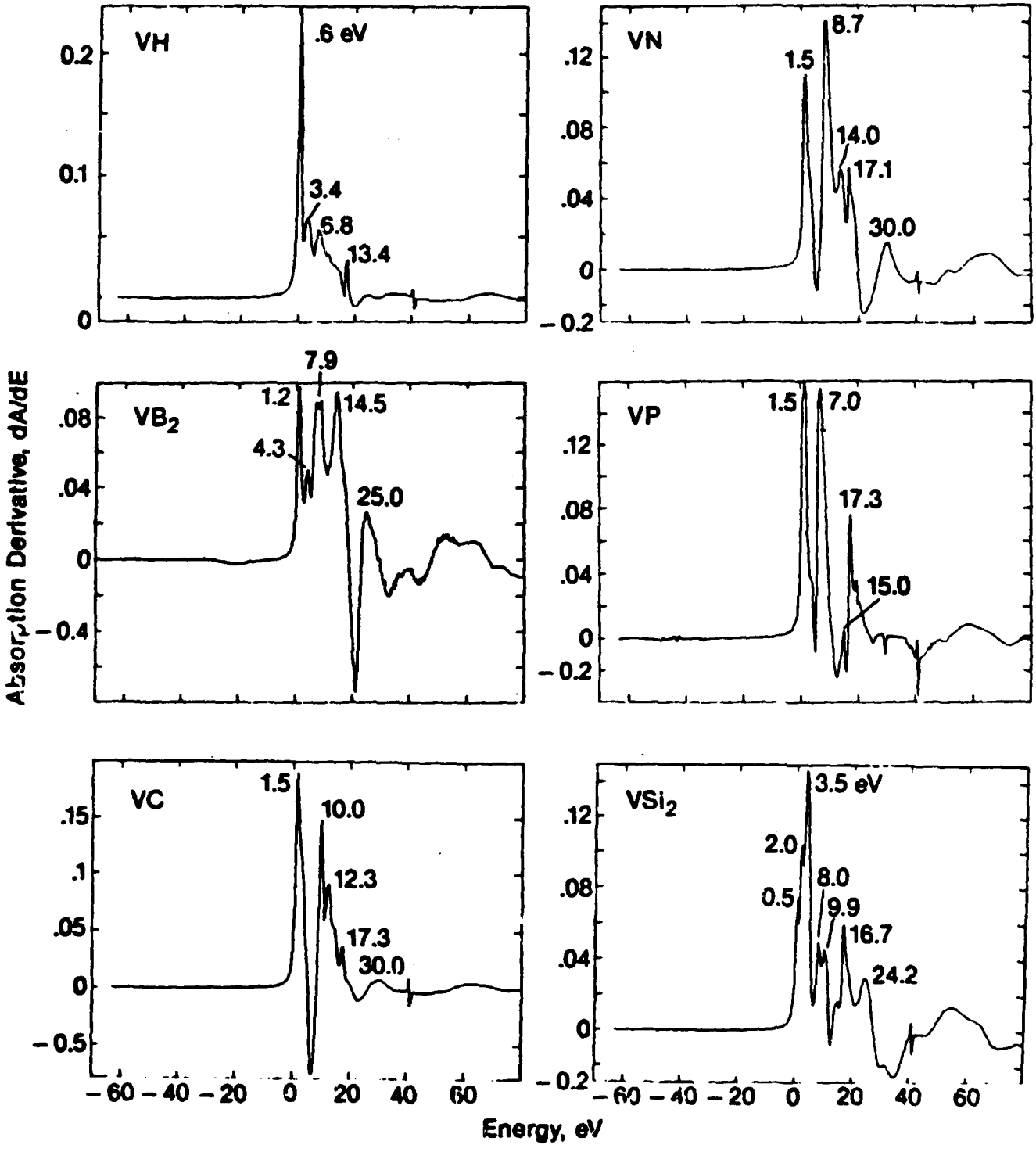
VH
.6 eV
3.4
6.8
13.4
VN
1.5
8.7
14.0
17.1
30.0
VB2
1.2
4.3
7.9
14.5
25.0
VP
1.5
7.0
17.3
15.0
VC
1.5
10.0
12.3
17.3
30.0
VSi2
0.5
2.0
3.5 eV
8.0
9.9
16.7
24.2
Absorption Derivative, dA/dE
Energy, eV

Fig. 13

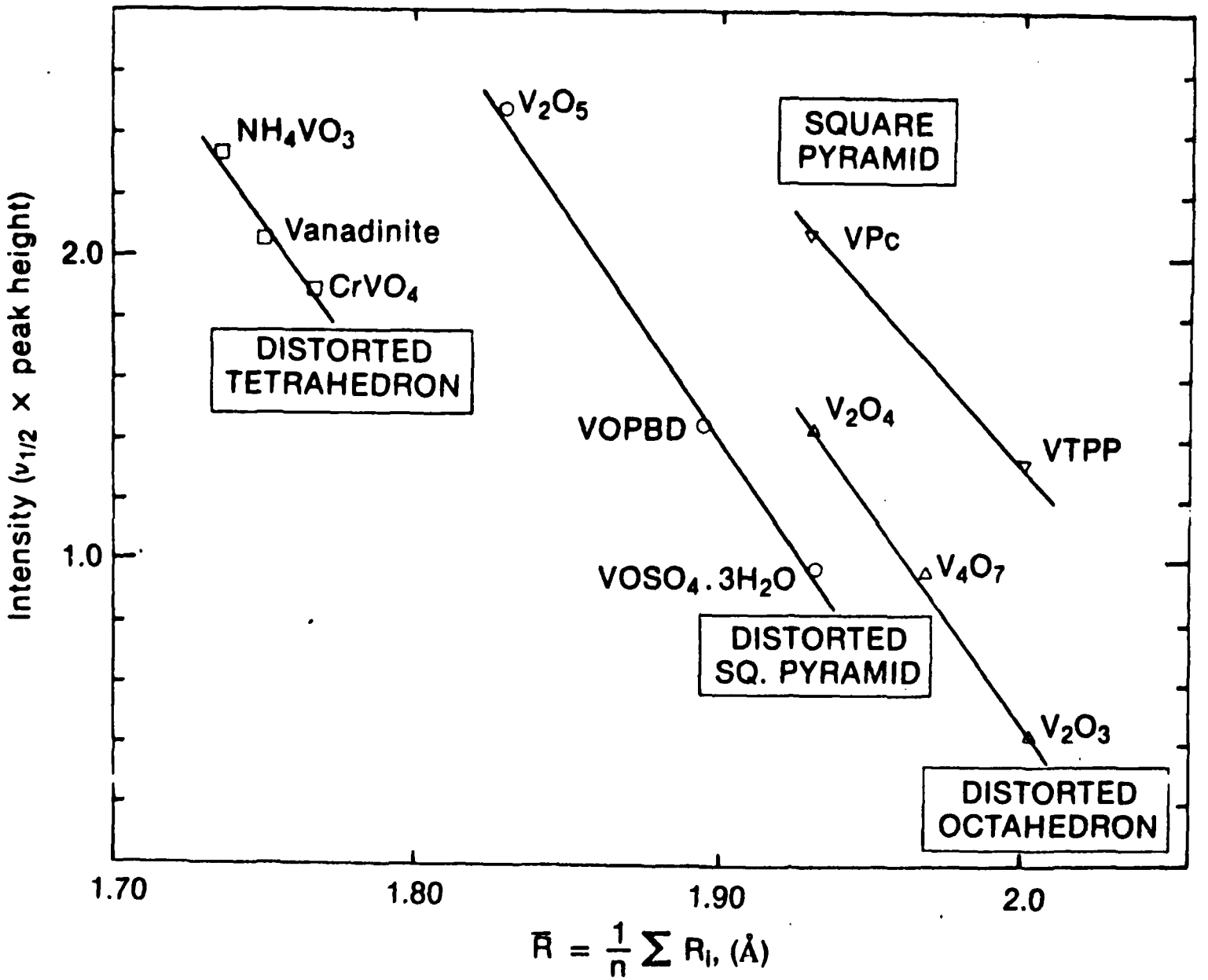
Intensity ($\nu_{1/2}$ × peak height)
2.0
1.0
1.70
1.80
1.90
2.0
$\bar{R} = \frac{1}{n}\sum R_i$, (Å)
NH_4VO_3
Vanadinite
$CrVO_4$
DISTORTED TETRAHEDRON
V_2O_5
SQUARE PYRAMID
VPc
VTPP
VOPBD
V_2O_4
$VOSO_4 . 3H_2O$
V_4O_7
DISTORTED SQ. PYRAMID
V_2O_3
DISTORTED OCTAHEDRON

Fig. 4

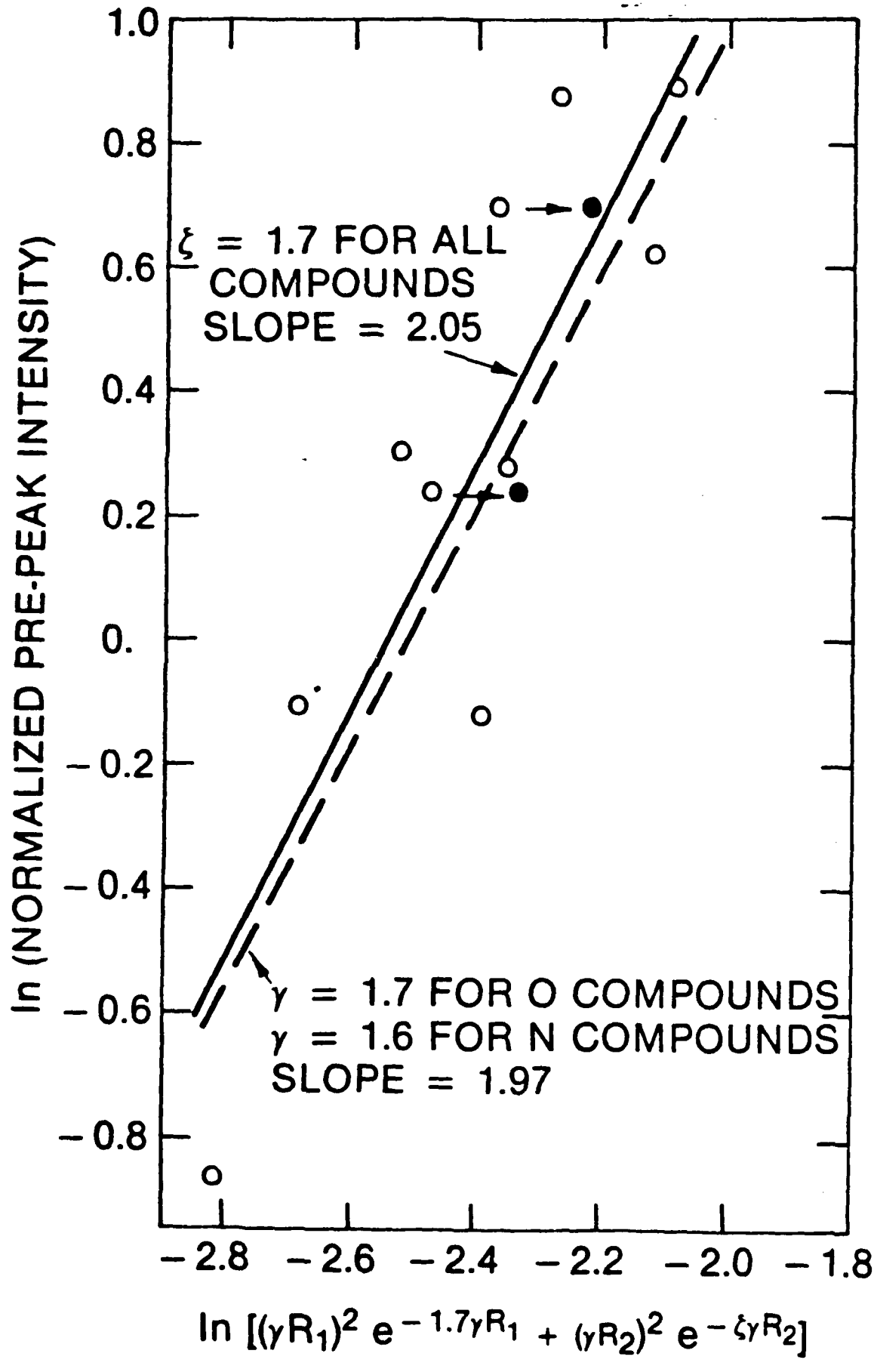
1.0
0.8
0.6
0.4
0.2
0.
−0.2
−0.4
−0.6
−0.8
ln (NORMALIZED PRE-PEAK INTENSITY)
ζ = 1.7 FOR ALL COMPOUNDS
SLOPE = 2.05
γ = 1.7 FOR O COMPOUNDS
γ = 1.6 FOR N COMPOUNDS
SLOPE = 1.97
−2.8
−2.6
−2.4
−2.2
−2.0
−1.8
ln [(γR1)2 e−1.7γR1 + (γR2)2 e−ζγR2]

Fig 15

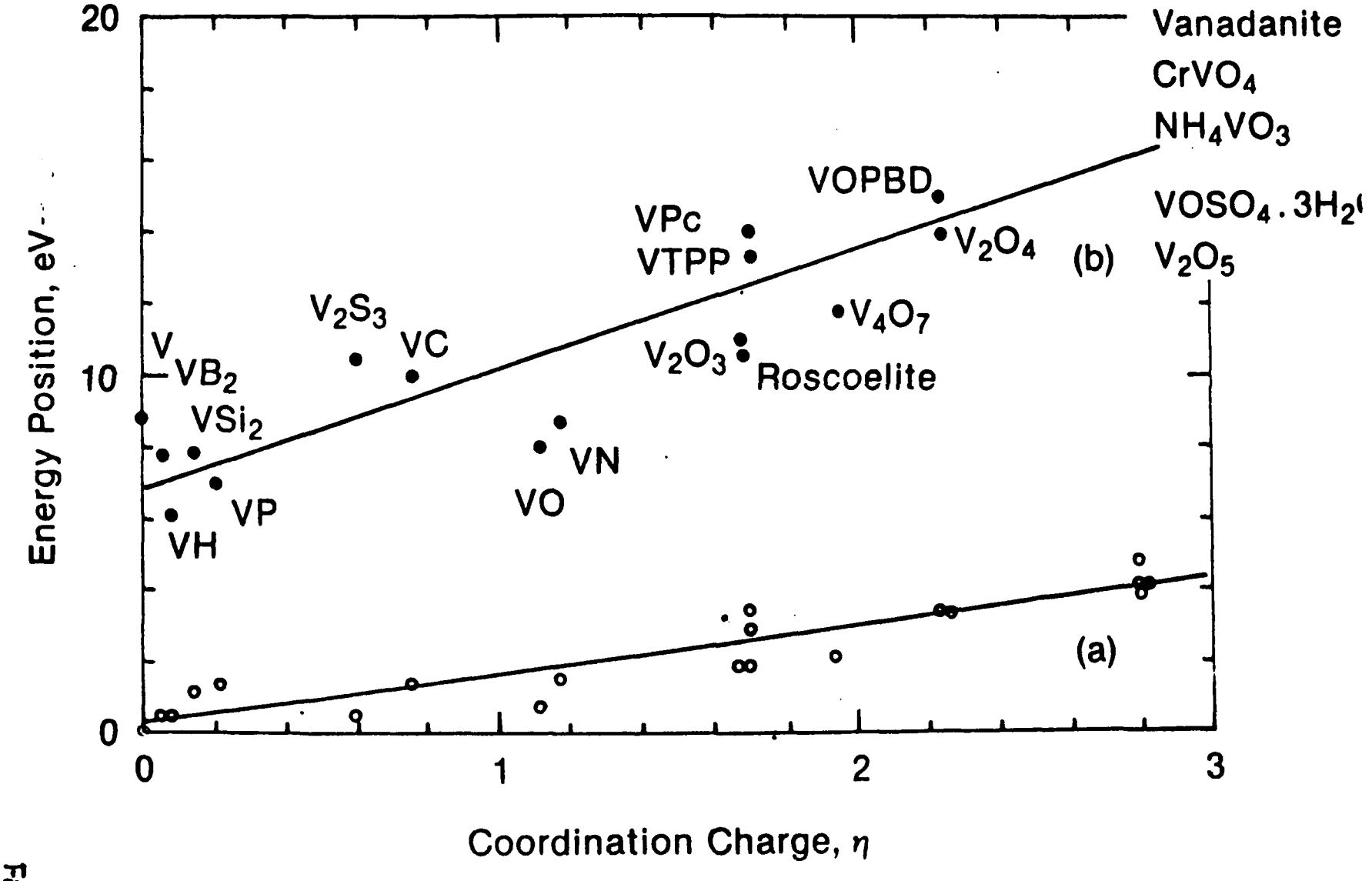
20
10
0
Energy Position, eV
0
1
2
3
Coordination Charge, η
Vanadanite
CrVO4
NH4VO3
VOSO4 . 3H2O
V2O5
VOPBD
V2O4
VPc
VTPP
(b)
V4O7
V2S3
VC
V
VB2
V2O3
Roscoelite
VSi2
VN
VO
VP
VH
(a)

Fig. 16

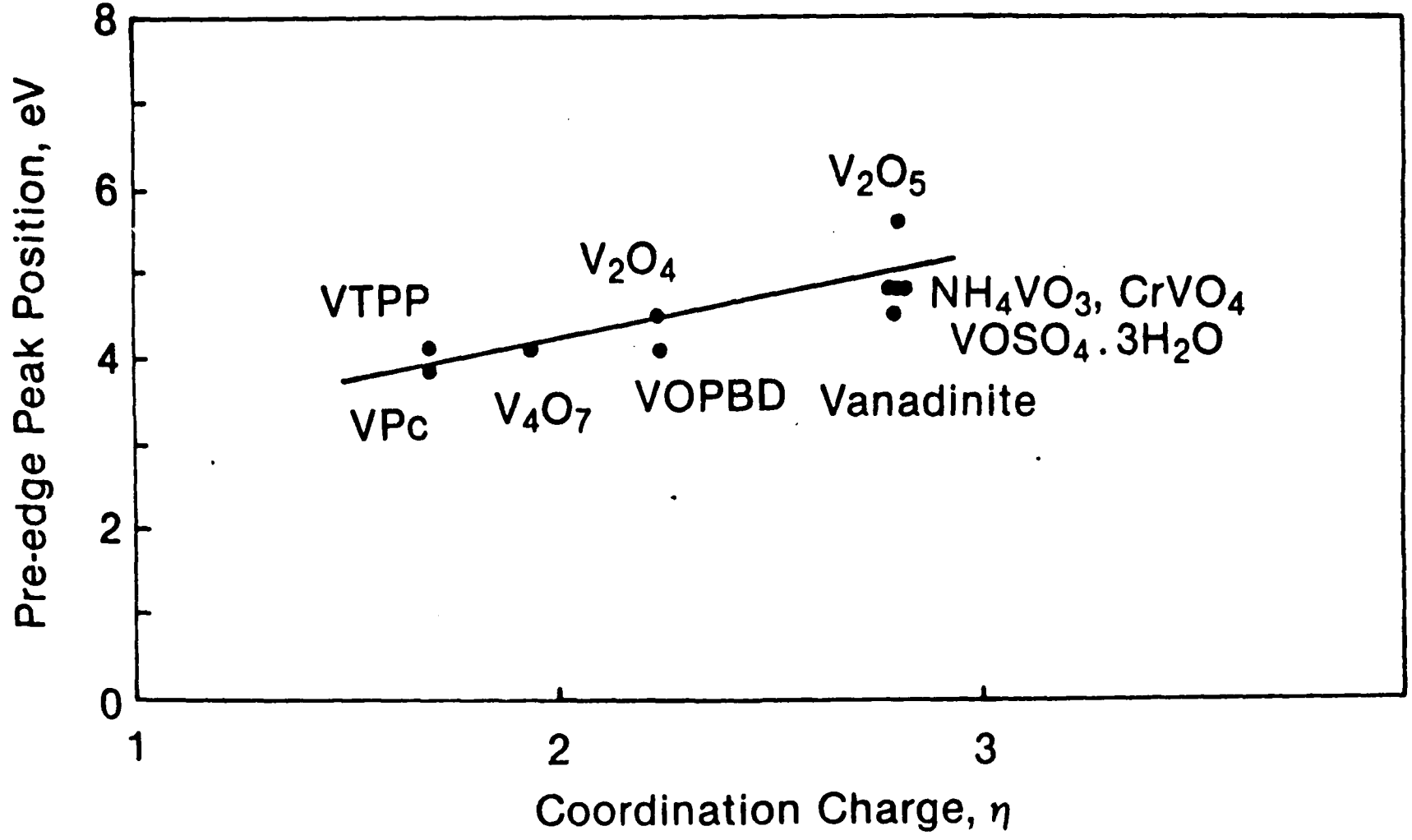
Pre-edge Peak Position, eV
8
6
4
2
0
1
2
3
Coordination Charge, η
V_2O_5
V_2O_4
VTPP
NH_4VO_3, $CrVO_4$
$VOSO_4 . 3H_2O$
VPc
V_4O_7
VOPBD
Vanadinite

Fig. 7

END

FILMED

2-85

DTIC